



Article

New Sulfanilamide Derivatives Incorporating Heterocyclic Carboxamide Moieties as Carbonic Anhydrase Inhibitors

Andrea Angeli^{1,2,*} , Victor Kartsev³, Anthi Petrou⁴ , Mariana Pinteala² , Roman M. Vydzhak⁵, Svitlana Y. Panchishin⁵ , Volodymyr Brovarets⁵, Viviana De Luca⁶ , Clemente Capasso⁶ , Athina Geronikaki^{4,*} and Claudiu T. Supuran¹

¹ Department of Chemistry “Ugo Schiff”, University of Florence, Via della Lastruccia 3-13, 50019 Sesto Fiorentino, Italy; claudiu.supuran@unifi.it

² Centre of Advanced Research in Bionanoconjugates and Biopolymers Department, “Petru Poni” Institute of Macromolecular Chemistry, 707410 Iasi, Romania; pinteala@icmpp.ro

³ InterBioScreen, Chernogolovka, 142432 Chernogolovka, Moscow Region, Russia; vkartsev@ibscreen.chg.ru

⁴ Department of Pharmacy, School of Health, Aristotle University of Thessaloniki, 54124 Thessaloniki, Greece; anthi.petrou.thessaloniki1@gmail.com

⁵ Department of Chemistry of Bioactive Nitrogen-Containing Heterocyclic Bases, V.P. Kukhar Institute of Bioorganic Chemistry and Petrochemistry, NAS of Ukraine 1, Murmanska St, 02094 Kyiv, Ukraine; rmvydzhak@gmail.com (R.M.V.); svpanch@ukr.net (S.Y.P.); brovarets@bpci.kiev.ua (V.B.)

⁶ Institute of Biosciences and Bioresources, CNR, Via Pietro Castellino 111, 80131 Napoli, Italy; viviana.deluca@ibbr.cnr.it (V.D.L.); clemente.capasso@ibbr.cnr.it (C.C.)

* Correspondence: andrea.angeli@unifi.it (A.A.); geronik@pharm.auth.gr (A.G.); Tel.: +30-230-199-7616 (A.G.)



Citation: Angeli, A.; Kartsev, V.; Petrou, A.; Pinteala, M.; Vydzhak, R.M.; Panchishin, S.Y.; Brovarets, V.; De Luca, V.; Capasso, C.; Geronikaki, A.; et al. New Sulfanilamide Derivatives Incorporating Heterocyclic Carboxamide Moieties as Carbonic Anhydrase Inhibitors. *Pharmaceuticals* **2021**, *14*, 828. <https://doi.org/10.3390/ph14080828>

Academic Editors: Susanna Nencetti, Nicolo Tonalì and Lidia Ciccone

Received: 19 July 2021

Accepted: 19 August 2021

Published: 23 August 2021

Publisher's Note: MDPI stays neutral with regard to jurisdictional claims in published maps and institutional affiliations.



Copyright: © 2021 by the authors. Licensee MDPI, Basel, Switzerland. This article is an open access article distributed under the terms and conditions of the Creative Commons Attribution (CC BY) license (<https://creativecommons.org/licenses/by/4.0/>).

Abstract: Carbonic Anhydrases (CAs) are ubiquitous metalloenzymes involved in several disease conditions. There are 15 human CA (hCA) isoforms and their high homology represents a challenge for the discovery of potential drugs devoid of off-target side effects. For this reason, many synthetic and pharmacologic research efforts are underway to achieve the full pharmacological potential of CA modulators of activity. We report here a novel series of sulfanilamide derivatives containing heterocyclic carboxamide moieties which were evaluated as CA inhibitors against the physiological relevant isoforms hCA I, II, IX, and XII. Some of them showed selectivity toward isoform hCA II and hCA XII. Molecular docking was performed for some of these compounds on isoforms hCA II and XII to understand the possible interaction with the active site amino acid residues, which rationalized the reported inhibitory activity.

Keywords: carbonic anhydrase; metalloenzymes; inhibitors; molecular docking

1. Introduction

Carbonic anhydrases (CAs) are a ubiquitous metalloenzyme family present in both eukaryote and prokaryote organisms [1]. To date, were discovered eight evolutionarily unrelated gene classes encoded as α -, β -, γ -, δ -, ζ -, η -, θ -, ι -CAs [2–8]. All these enzymes promoting the hydration of carbon dioxide (CO₂) to bicarbonate (HCO₃[−]) and protons (H⁺) following a two-step catalytic mechanism [9]. In humans, all CAs belong to the α -class with fifteen isoforms differing by molecular features, oligomeric arrangement, cellular localization, distribution in organs and tissues, expression levels, kinetic properties, and response to different classes of inhibitors [10–12]. To date, twelve catalytic active isoforms (CA I–IV, VA–VB, VI–VII, IX, and XII–XIV) are known, with a variable CO₂ hydrase activity, which play pivotal roles in a variety of physiological processes connected to pH and CO₂ homeostasis, respiration, electrolyte secretion, biosynthetic reactions (i.e., gluconeogenesis, lipogenesis, and ureagenesis), bone resorption; calcification; and tumorigenicity [13]. On the other hand, abnormal levels or activities of these enzymes have been often associated with different human diseases, some of which have been clinically exploited and validated as therapeutic targets for the treatment or prevention of various pathologies such

as glaucoma, edema, neurological disorders, epilepsy and more recently cancer [14–16]. In this context, many efforts are made to explore novel and selective Carbonic Anhydrase Inhibitors (CAIs) leading compounds with potential biomedical applications [17,18]. Some of the CA inhibitors mentioned in ChEMBL are presented in Figure 1.

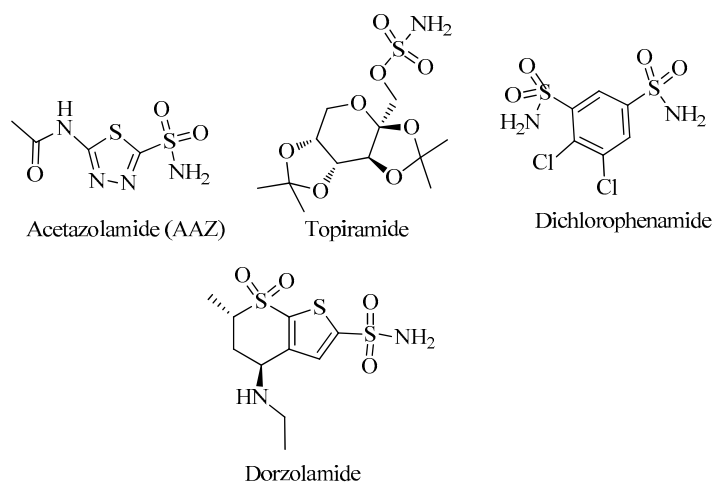


Figure 1. Known CA inhibitors.

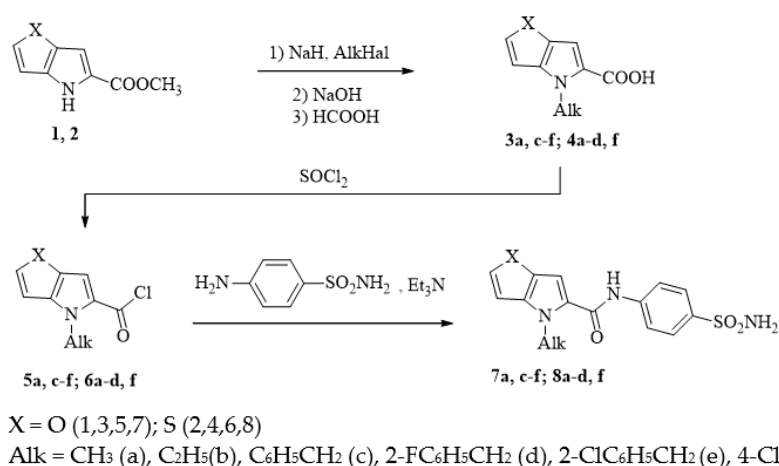
In addition, furano- and thienopyrroles have attracted interest of medicinal chemists due to their wide range of biological activities, such as antiviral [19–21], antimicrobial [22–24], anticancer [25–27], anti-inflammatory [28,29], antidiabetic [30], carbonic anhydrase inhibitory [31]. On the other hand, some sulfonamides also show anticancer [32,33], antimicrobial [34,35], anti-inflammatory [36,37] antidiabetic [38], and antitubercular [39] activities.

Taking into account all of the mentioned above, here we report the synthesis of *N*-(4-sulfamoylphenyl)-4*H*-thieno[3,2-*b*]pyrrole-5-carboxamide and *N*-(4-sulfamoylphenyl)-4*H*-furan[3,2-*b*]pyrrole-5-carboxamide derivatives incorporating into one scaffold carboximide and sulfonamide moieties. Furthermore, 6-oxo[1,3]thiazolo[3,2-*b*][1,2,4]triazole derivatives were also synthesized. The experimental studies were developed together with in silico techniques, aimed to propose a reliable binding disposition for this class of CAIs.

2. Results and Discussion

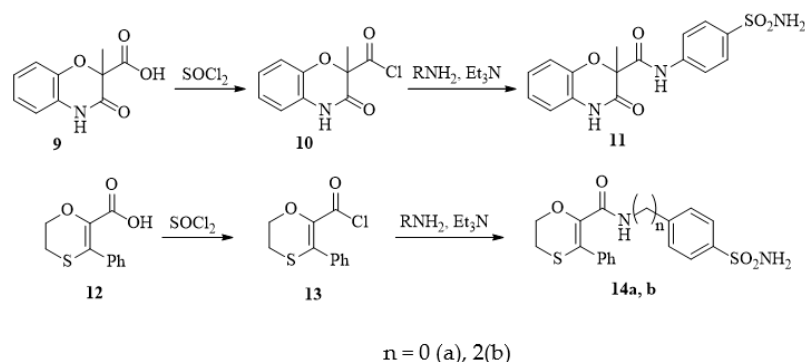
2.1. Design and Synthesis of Compounds

The synthesis of target sulfonamides **7a,c,f** and **8a-d,f** is presented in Scheme 1. Intermediate esters were obtained by alkylation of the starting compounds **1** [40] or **2** [41] with the appropriate alkyl halides in DMF using sodium hydride as a base. Then, these compounds were used without additional purification to prepare 4-alkyl-4*H*-furo[3,2-*b*]pyrrole-5-carboxylic acids **3a,c,f** and 4-alkyl-4*H*-thieno[3,2-*b*]pyrrole-5-carboxylic acids **4a-d,f**. Acyl chlorides **5** and **6** were obtained (with yields of 50–80%) by the treatment of carboxylic acids **3** and **4** with thionyl chloride in toluene. Relatively unstable compounds **5** and **6** were immediately used for the further step of preparation of the *N*-[4-(aminosulfonyl)phenyl]-4-alkyl-4*H*-furo[3,2-*b*]pyrrole-5-carboxamides **7a,c,f** and *N*-[4-(aminosulfonyl)phenyl]-4-alkyl-4*H*-thieno[3,2-*b*]pyrrole-5-carboxamides **8a-d,f**.



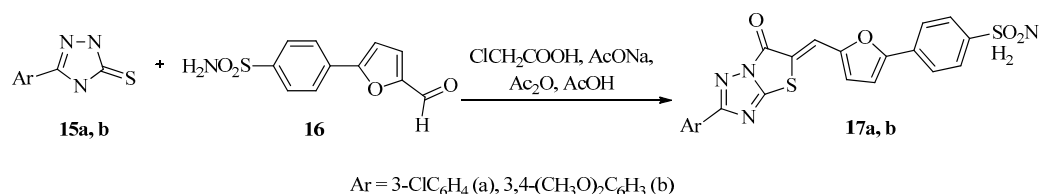
Scheme 1. Synthesis of furo[3,2-*b*]pyrrole and thieno[3,2-*b*]pyrrole derivatives.

Synthesis of amides **11** and **14a,b** is shown in Scheme 2. 2-Methyl-3-oxo-3,4-dihydro-2*H*-1,4-benzoxazine-2-carboxylic acid **9** [42] and 3-phenyl-5,6-dihydro-1,4-oxathiine-2-carboxylic acid **12** [43] were converted into acid chlorides **10** and **13**, which without further purification upon reaction with corresponding amines led to **11** and **14a,b**.



Scheme 2. Synthesis of amides **11** and **14a,b**.

6-Oxo[1,3]thiazolo[3,2-*b*][1,2,4]triazole derivatives **17a,b** were synthesized according to pathway shown on Scheme 3. Compounds **17a,b** were obtained with high yields starting from 5-aryl-2,4-dihydro-3*H*-1,2,4-triazole-3-thiones **15a,b** [44] and 4-(5-formyl-2-furyl)-benzenesulfonamide **16** [45] according to the earlier proposed procedure [46–48].



Scheme 3. Synthesis of substituted 6-Oxo[1,3]thiazolo[3,2-*b*][1,2,4]triazole.

The structure and composition of compounds **3a,c-f**, **4a-d,f**, **7a,c-f**, and **8a-d,f** were confirmed by ¹H-NMR, ¹³C-NMR spectroscopy, and elemental analysis (Supplementary Materials) Thus, the signal of the carboxyl group of compounds **3**, **4**, and **7** were found as a singlet in the range of 10.0–10.4 ppm. The signals of the 4*H*-furo[3,2-*b*]pyrrole moiety of compounds **3** and **7** were observed at 7.70–7.80 ppm, while the signals of the 4*H*-thieno[3,2-*b*]pyrrole moiety of the compounds **4** and **8** at 7.50–7.60 ppm. The sulfonamide group was observed as a singlet at 7.20–7.30 ppm. On the other hand in the case of compounds **11**

and **14a,b** NH protons signals were found as two singlets at 10.91 ppm and 10.49 ppm, while the signal of the sulfonamide group was as a singlet at 7.24 ppm. The peak of the methyl group appears as a singlet at 1.73 ppm, while of the methylenidene group of **17a,b** CH= protons appear as a singlet at 8.20–8.10 ppm, deshielded by adjacent C=O group, at higher chemical shift values, indicating a predominant existence of Z-configuration of this group double bond in these compounds. The expected ones for E isomer have methine proton with a lesser deshielding effect [49,50].

2.2. Carbonic Anhydrase Inhibition

All compounds, here reported, were evaluated for their inhibitory activity against four human CA isoforms, namely: hCA I, hCA II, hCA IX, and hCA XII. The results are shown in Table 1.

Table 1. Inhibition data of human CA isoforms I, II, IX, and XII with compounds **7a-f**, **8a-f**, **11,14a-b**, **17a-b**, and **AAZ** by a stopped-flow CO₂ hydrase assay [51].

Cmp	K _i (nM) *			
	hCA I	hCA II	hCA IX	hCA XII
7a	717.9	8.4	103.2	6.9
7c	3563	37.5	275.6	4.6
7e	858.3	23.8	239.5	19.6
7f	878.1	34.3	187.2	37.2
8a	664.6	8.8	66.6	30.7
8b	269.7	6.8	250.8	5.1
8c	399.5	8.9	140.5	7.8
8d	656.3	8.7	171.3	8.2
8f	699.2	68.1	81.4	8.9
11	70.6	6.5	259.8	5.3
14a	56.5	6.7	280.5	6.1
14b	71.2	7.4	155.2	6.6
17a	2925	44.7	320.0	7.6
17b	918.5	59.4	252.9	40.2
AAZ	250	12.1	25.7	5.7

* Mean from 3 different assays, by a stopped-flow technique (errors were in the range of ±5–10% of the reported values).

According to obtained results it is obvious that all compounds displayed inhibition against all tested hCA isoforms, but with different range of inhibition constants. Thus, the K_i values of compounds against hCA I ranged from 56.5 to 918.5 nM, with compound **14a** exhibiting the best activity (K_i = 56.5 nM). Good activity was achieved also for compound **11** with K_i value of 70.6 nM, followed by compound **14b** (K_i = 71.2 nM) compared to **AAZ** (K_i = 250 nM). The lowest activity against hCA I was observed for compound **17b** with K_i values at 918.5 nM. The order of activity of compounds against hCA I can be presented as follows: **14a** > **11** > **14b** > **8b** > **8c** > **8d** > **8a** > **8f** > **7a** > **7e** > **7f** > **17b** > **17a** > **7c**.

The structure–activity relationship studies revealed that the presence of 3-phenyl-5,6-dihydro-1,4-dioxine-2-carboxamide (**14a**) as a substituent at the para- position of benzenesulfonamide is very beneficial for inhibitory activity against hCA I. It replacement by 2-methyl-3-oxo-3,4-dihydro-2H-benzo[b][1,4]oxazine-2-carboxamide led to compound **11** with decreased activity. The introduction to position 4 of the benzenesulfonamide 3-phenyl-N-propyl-5,6-dihydro-1,4-oxathiine-2-carboxamide substituent with prolonged chain between benzenesulfonamide and 5-phenyl-2,3-dihydro-1,4-oxathiine **14b** did not affect the activity much, only decreasing it slightly. Among furo- and thieno- derivatives it is obvious that in general thieno- derivatives are more potent inhibitors against hCA I than furo-, which are the least active (**7a**, **7e**, **7f**, and **7c**). Among N-(4-sulfamoylphenyl)-4H-thieno[3,2-b]pyrrole-5-carboxamide derivatives the presence of ethyl group on position 4 of N-(4-sulfamoylphenyl)-4H-thieno[3,2-b]pyrrole (**8b**) appeared to be beneficial. Replacement of ethyl by benzyl (**8c**) decreased a little activity, followed by 2-fluorobenzyl substituent (**8d**). The less active among thieno derivatives were found to be compound

with 4-chlorobenzyl substituent, followed by four furo derivatives with the 4-benzyl-*N*-(4-sulfamoylphenyl)-4*H*-furo[3,2-*b*]pyrrole-5-carboxamide exhibiting the lowest inhibitory activity against hCA I isoform.

It is worth noticing that in general, these compounds showed better activity toward cytosolic hCA II isoform than against almost all other isoforms with K_i values in the range of 6.5–68.1 nM. Thus, the order of activity against hCA II isoform can be presented as **11** > **14a** > **8b** > **14b** > **7a** > **8d** > **8a** > **8c** > **7e** > **7f** > **7c** > **8f** > **17a** > **17b**. The highest activity was achieved for compound **11** with K_i = 6.5 nM, followed by **14a** (K_i = 6.7 nM) compared to **AAZ** with a K_i value of 12.1 nM. It is interesting to notice that the most active compounds against hCA I isoform were also active against hCA II isoform. It should be mentioned that compound **8a** was the most selective one with a selectivity index (SI) 75.5 towards hCA I, 7.6 compared to hCA IX, and 3.5 to hCA XII isoforms. Eight compounds exhibited higher activity against the cytosolic hCA II isoform than reference compound **AAZ**.

According to structure-activity relationship studies, the presence of 2-methyl-3-oxo-3,4-dihydro-2*H*-benzo[*b*][1,4]oxazine-2-carboxamide substituent on position 4 of benzenesulfonamide (**11**) was positive for inhibitory activity against hCA II isoform. The replacement it by 3-phenyl-5,6-dihydro-1,4-dioxine-2-carboxamide (**14a**) decreased a little the activity followed by 4-ethyl-4*H*-thieno[3,2-*b*]pyrrole-5-carboxamide (**8b**). The less potent inhibitor was, as in the case with hCA I isoform, thieno derivative 4-(4-chlorobenzyl)-*N*-(4-sulfamoylphenyl)-4*H*-thieno [3,2-*b*]pyrrole-5-carboxamide (**8f**).

As far as hCA IX isoform is concerned, the new compounds showed moderate to weak inhibitory activity with K_i in the range of 81.4–320.0 nM compared to 25.7 nM of acetazolamide.

In the case of the hCA XII isoform, these compounds exhibited much better activity than against hCA IX and hCA I isoforms but were less effective compared to their activity on hCA II. Their K_i was in the range of 4.6–37.2 nM. The activity in descending order can be presented as follows: **7c** > **8b** > **11** > **14a** > **14b** > **7a** > **17a** > **8c** > **8d** > **8f** > **7e** > **8a** > **7f** > **17b**. Three compounds (**7c**, **8b**, **11**) exhibited activity better than that of **AAZ** with compound **7c** displaying the highest activity (K_i = 4.6 nM) compared to **AAZ** (K_i = 5.7 nM). The lowest activity was shown by furo derivative **7f** (K_i = 37.2 nM). It is interesting to notice that compound **7c** (4-benzyl-*N*-(4-sulfamoylphenyl)-4*H*-furo[3,2-*b*]pyrrole-5-carboxamide) demonstrated the highest activity against the hCA XII isoform, being the less active against the hCA I and hCA II isoforms.

The structure-activity relationship studies revealed that the presence of 4-benzyl-4*H*-furo[3,2-*b*]pyrrole-5-carboxamide plays a positive role in inhibitory activity against the hCA XII isoform. Replacement of furan by thieno ring and benzyl by ethyl led to compound **8b** with slightly lower activity, while the introduction to position 4 of benzenesulfonamide 2-methyl-3-oxo-3,4-dihydro-2*H*-benzo[*b*][1,4]oxazine-2-carboxamide substituent (**11**) decreased more the activity. On the other hand, the presence of 4-(4-chlorobenzyl)-4*H*-furo[3,2-*b*]pyrrole-5-carboxamide as a substituent on benzenesulfonamide moiety appeared to be detrimental for hCA XII inhibitory activity. Finally, compounds **11**, **14a**, **14b** were found to be active against three hCA I, hCA II, and hCA XII isoforms.

2.3. Molecular Docking Studies

In an attempt to predict the probable inhibition mechanism of the tested compounds, molecular docking studies were performed. As a representative of the whole set of compounds, ligands **7c**, **8a**, **8b**, **11**, and **14a** were selected for docking studies. All human CAs isoforms have similar active site architecture. Their active site contains three conserved His94, His96, and His119 residues acting as zinc ligands and another two conserved residues that act as “gatekeepers” Thr199 and Glu105 [51–53]. However, these isoforms vary in the residues generally in the middle and to the exit of the active site cavity. The results of molecular docking studies of the tested compounds on hCA I, II, IX, and XII isoforms are presented in Table 2 and revealed that all tested compounds bind the enzymes,

chelating the Zn (II) ion of the active site, in a deprotonated form, as anions (negative nitrogen of the sulfonamide group) [54].

Table 2. Molecular docking free binding energies (kcal/mol) and interactions of tested compounds on hCA I, II, IX, and XII isoforms.

No	hCA Isoform	Estimated Free Binding Energy (Kcal/mol)	Chelating the Zn (II) Ion	Residues Involved in H-Bond Interactions	Residues Involved in Hydrophobic Interactions
7c	hCA I	−5.47	No	-	Ala121, Ala135
	hCA II	−7.11	Yes	Thr199	Ile91
	hCA IX	−6.80	Yes	Thr199	Val121, Thr200
	hCA XII	−11.32	Yes	His67, Gln92, Thr200	Leu198
8a	hCA I	−6.88	Yes	Thr199	Ala135, Leu198
	hCA II	−8.95	Yes	His94, Thr199	Ile91, Phe131, Thr200
	hCA IX	−7.91	Yes	Thr199	Val121, Thr200
	hCA XII	−6.42	Yes	-	Val121, Leu198
8b	hCA I	−8.17	Yes	Gln92	Ala121, Leu198
	hCA II	−9.24	Yes	His94, Thr199	Val121, Phe131, Leu198
	hCA IX	−6.54	Yes	Thr199	Val121, Leu198
	hCA XII	−9.80	Yes	Gln92, His94, Thr200	Val121, Ala131, Leu198
11	hCA I	−9.91	Yes	Gln92, Thr199	Leu131, Ala132, Thr202
	hCA II	−9.24	Yes	His94, Thr200	Val121, Phe131, Leu198
	hCA IX	−6.20	Yes	-	Val121, Val131, Leu198
	hCA XII	−9.78	Yes	His94, Thr200	Val121, Val143, Ala131, Leu198
14a	hCA I	−11.02	Yes	His67, Thr199	Ala121, Ala132, Leu198
	hCA II	−9.15	Yes	Asn67, Thr199	Ile191, Val121, Phe131, Leu198, Thr200
	hCA IX	−6.51	Yes	Thr199	Val121, Thr200
	hCA XII	−9.42	Yes	Thr200	Val121, Leu198
AAZ	hCA I	−8.28	Yes	Gln92	Leu198, Thr199, His200, Pro201, Trp209
	hCA II	−8.87	Yes	Thr199, Thr200	Val121, Phe131, Leu198, Trp209
	hCA IX	−9.02	Yes	Thr199, Thr200	Val121, Val143, Val131, Leu198, Trp209
	hCA XII	−9.14	Yes	Thr199, Thr200	Val121, Val143, Leu198, Trp209

According to docking studies, the selectivity and the inhibition profile of some compounds to each isoform are depending on the differences in the active sites of the enzymes. More specifically, their inhibition profile is affected by the nature of the amino acids of the active site of the enzymes which determinate the conformation and interactions that compounds will adopt within the enzyme active site. For instance, compound 7c, which has a K_i for the hCA II enzyme of 37.5 nM and a lower K_i for hCA XII of 4.6 nM, adopts different conformations when binding both hCAs. The main reason is probably the presence of the bulky hydrophobic residue Phe131 in the hCA II enzyme, unlike the smaller residue Ala131 in hCA XII. This smaller residue in the hCA XII enzyme, allows ligands to freely enter the active site of the enzyme and to adopt a conformation that favors interactions with residues in the hydrophobic pocket and increases the selectivity of the compound to this isoform (Figure 2). Moreover, the superposition of the two structures of hCAs bound to compound 7c revealed this steric hindrance of the bulky residue Phe131 (Figure 2A). Consequently, 7c adopts a different conformation within the active site of the hCA II enzyme with the benzene ring being removed away from the bulky Phe131, interacting less with the residues of the active site of the enzyme and forming a less stable complex ligand-enzyme. This is probably the reason that explains the higher experimental K_i of this compound for isoform hCA II. Furthermore, compound 7c forms a hydrogen bond between the sulfonamide and the backbone of Thr199 of both isoforms and two more H-bonds between its carboxyl group and the backbones of residues Gln92 and Lys67 of isoform hCA XII, which further stabilize

the complex ligand hCA XII and explains the high inhibition potency of the compound against this isoform (Figure 2B,C, Table 2).

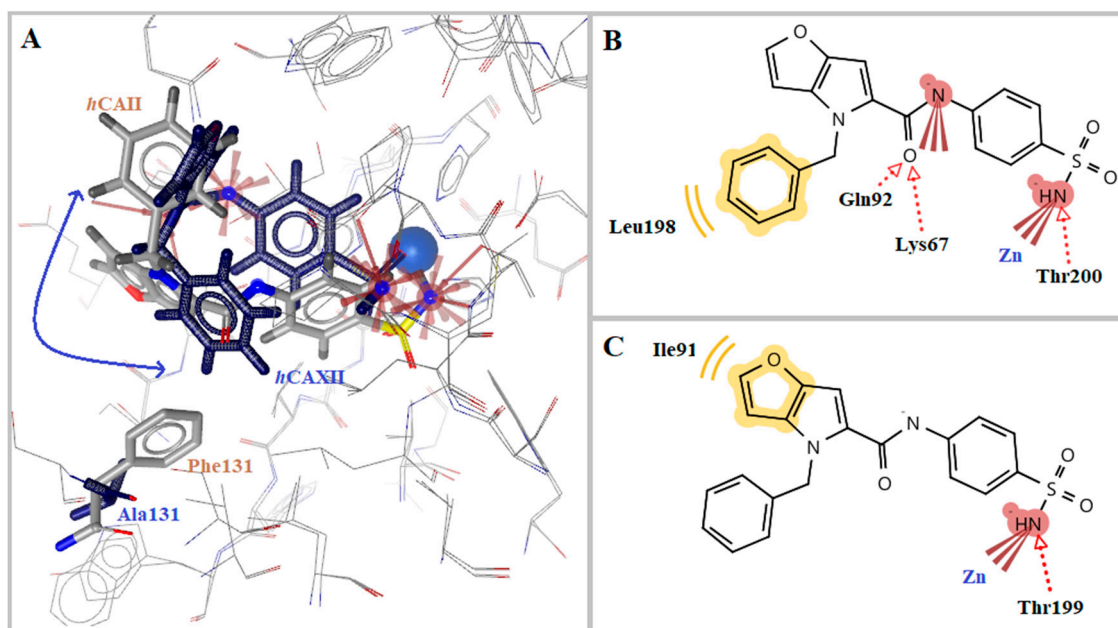


Figure 2. (A) Superposition of compound 7c bound to hCA II (grey) in comparison to hCA XII (blue), with specific residues labeled. (B) 2D interaction diagram of compound 7c docking pose interactions with the key amino acids in hCA XII and (C) in hCA II, Active site zinc is shown as a blue sphere, red dotted arrows indicate H-bond and yellow spheres hydrophobic interactions. Blue double-headed arrow indicates the direction of conformational change of the compound bound to hCA II in comparison to the hCA XII enzyme.

On the other hand, compounds **8a** and **8b** (Figure 3) differ from compound **7c** by the presence of methyl and ethyl substituent instead of benzene (**7c**) on the indole ring. Both these substituents provide flexibility to the compounds, making them able to avoid the steric hindrance with the bulky residue Phe131 of hCA II isoform, increasing the inhibition potency. However, these compounds can also inhibit the hCA XII isoform. This is illustrated in Figure 4 where compound **8b** in both hCA II and hCA XII isoforms is adopting a conformation that favors the interactions with both active sites of the isoforms, increasing the stability of the complex and consequently the inhibition potency of the compound (Figure 4A). The negative nitrogen of the sulphonamide group coordinates to the Zn (II) ion and forms a hydrogen bond with conserved residue His94. In the hCA II isoform, both oxygen atoms of the sulphonamide group formed two hydrogen bonds interacting with the conserved residue Thr199, while in isoform hCA XII only one hydrogen bond with residue Thr200 is formed. Moreover, the ethyl substituent is interacting hydrophobically with Phe131 and Ala131 of hCA II and hCA XII isoforms respectively. Hydrophobic interactions between the benzene moiety and the residue Leu198 and Val121 in both isoforms (Figure 4B,C, Table 2) were also observed. These interactions stabilize further the complex ligand-enzyme and positively impacting into the inhibition profile of the compounds.

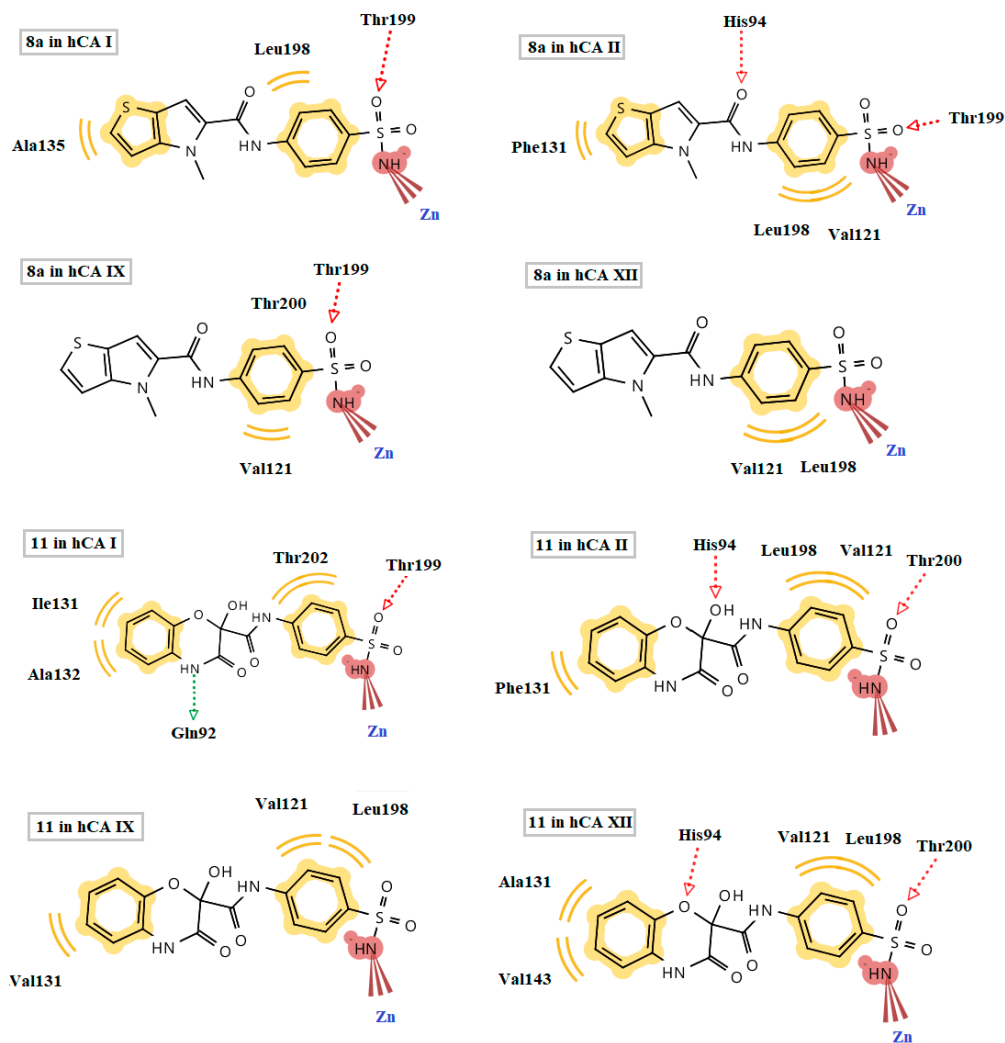


Figure 3. 2D interaction diagrams of compounds **8a** and **11** docking poses interactions with the key amino acids in hCA I, hCA II, hCAIX, hCA XII.

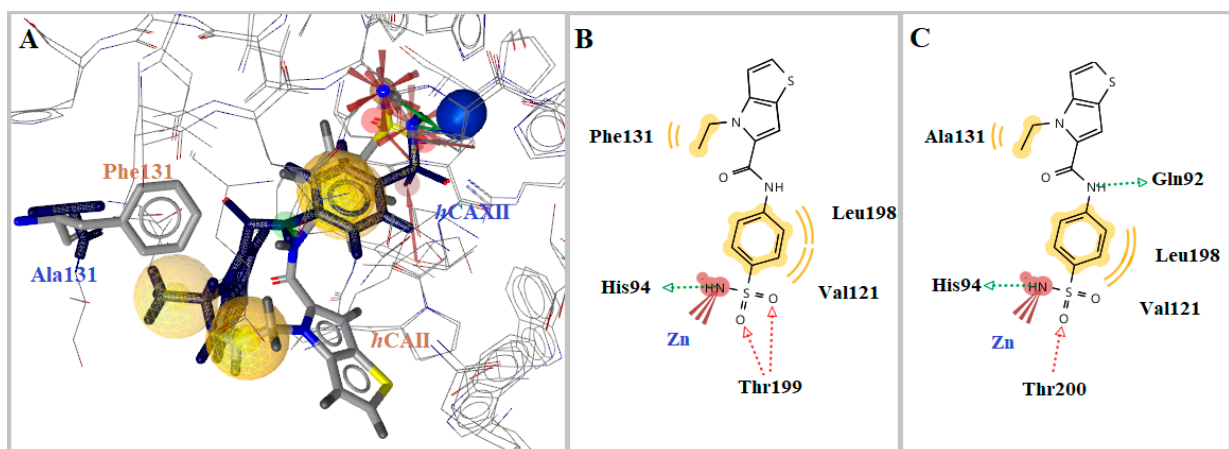


Figure 4. (A) Superposition of compound **8b** bound to hCA II (grey) in comparison to hCA XII (blue), with specific residues labeled, (B) 2D interaction diagram of compound **8b** docking pose interactions with the key amino acids in hCA II and (C) in hCA XII. Active site zinc is shown as a blue sphere, red dotted, and green arrows indicate H-bond and yellow spheres hydrophobic interactions.

On the other hand, docking of compound **14a** into the active site of all CA isoforms revealed the probable reason for its good inhibition profile. As it is presented in Figure 5, compound **14a** binds hCA I and hCA II isoform in the same manner as **AAZ**, with the negative nitrogen of the sulphonamide group chelating the Zn(II) ion. Moreover, in the hCA II isoform the benzene moiety of the compound interacts hydrophobically with residues Phe131 and Ile91. These interactions increase the stability of the complex and probably explain its lower K_i than that of **AAZ** (6.7 nM vs. 12.1 nM).

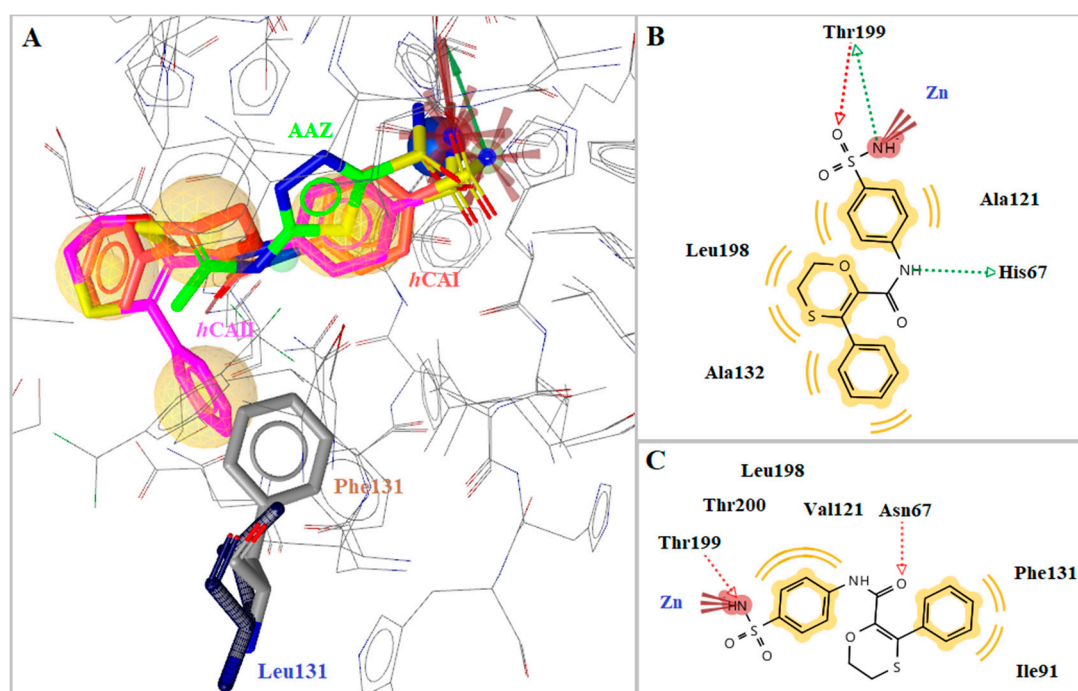


Figure 5. (A) Superposition of compound **14a** bound to hCA I (orange) in comparison to hCA II (magenta) and **AAZ** (green) in hCA I, (B) 2D interaction diagram of compound **14a** docking pose interactions with the key amino acids in hCA I, (C) in hCA II. Active site zinc is shown as a blue sphere, red dotted and green arrows indicate H-bond and yellow spheres hydrophobic interactions.

2.4. In Silico Prediction Studies

Drug likeness is examined as an important tool that provides the base for the molecules to be a powerful drug candidate. The number of violations to various rules viz. Lipinski, Ghose, Veber, Egan, and Muegge [55–60], along with bioavailability and Drug-likeness scores are given in Table 3. The results showed that none of the compounds violated any rule and their bioavailability score was around 0.55. All compounds exhibited moderate to good Drug-likeness scores ranged from -0.58 to 1.00 . Moreover, the bioavailability radar of some of the compounds is displayed in Figure 6. The compound **8f** appeared to be the best in the in-silico predictions with a Drug-likeness score of 1.00 without any rule violation.

Table 3. Drug likeness predictions and Physicochemical-Pharmacokinetic/ADME properties of tested compounds.

No	MW	Number of HBA ^a	Number of HBD ^b	Log P _{o/w} (iLOGP) ^c	Log S ^d	TPSA ^e	BBB permeant ^f	Lipinski, Ghose, Veber, Egan, and Muegge Violations	Bioavailability Score	Drug-Likeness Model Score
7a	319.3	5	2	1.30	Moderately soluble	115.71	No	0	0.55	0.57
7c	395.4	6	2	1.79	Poorly soluble	115.71	No	0	0.55	0.44
7e	429.9	5	2	2.05	Poorly soluble	115.71	No	0	0.55	0.36
7f	429.9	5	2	2.26	Poorly soluble	115.71	No	0	0.55	0.97
8a	335.4	4	2	1.72	Moderately soluble	130.81	No	0	0.55	0.59
8b	349.4	4	2	2.02	Moderately soluble	130.81	No	0	0.55	0.80
8c	411.5	4	2	2.17	Poorly soluble	130.81	No	0	0.55	0.47
8d	429.5	5	2	1.84	Poorly soluble	130.81	No	0	0.55	0.21
8f	445.9	4	2	2.49	Poorly soluble	130.81	No	0	0.55	1.00
11	484.9	7	1	2.90	Poorly soluble	157.18	No	0	0.55	-0.58
14a	510.6	9	1	3.10	Poorly soluble	175.64	No	1 (MW > 500)	0.55	-0.53
14b	36.4	6	3	1.19	Moderately soluble	135.97	No	0	0.55	0.14
17a	376.5	5	2	1.74	Moderately soluble	132.17	No	0	0.55	0.45
17b	404.5	5	2	2.50	Poorly soluble	132.17	No	0	0.55	0.37

^a number of hydrogen bond acceptors; ^b number of hydrogen bond donors; ^c lipophilicity; ^d Water solubility (SILICOS-IT [S = Soluble]); ^e topological polar surface area (Å²); ^f Blood-Brain Barrier permeant.

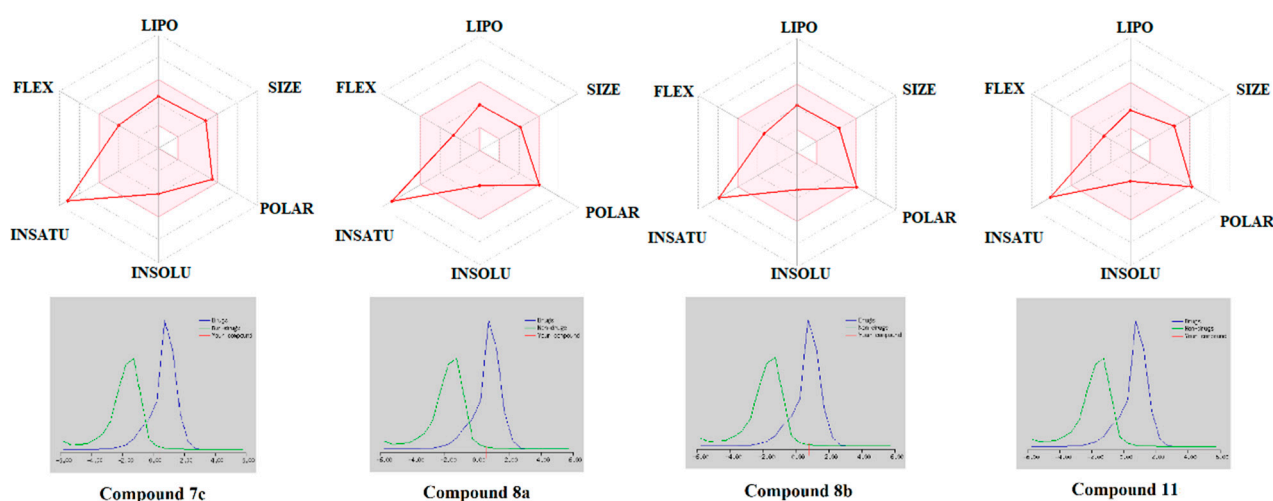


Figure 6. Bioavailability Radar of the tested compounds. The pink area represents the optimal range for each property for oral bioavailability, (Lipophilicity (LIPO): XLOGP3 between -0.7 and $+5.0$, Molecular weight (SIZE): MW between 150 and 500 g/mol, Polarity (POLAR) TPSA between 20 and 130 Å², Solubility (INSOLU): log S not higher than 6, Saturation (INSATU): fraction of carbons in the sp³ hybridization not less than 0.25, and Flexibility (FLEX): no more than 9 rotatable bonds.

3. Materials and Methods

3.1. General

The solvents were purified according to the standard procedures. The ¹H, ¹³C spectra were recorded on a Varian Unityplus-400 spectrometer (400 and 125 MHz, respectively) in a DMSO-*d*₆ solution. Chemical shifts are reported in ppm downfield from TMS as internal standards. Mass spectra were recorded on an LC-MS instrument with chemical ionization (CI). LC-MS data were acquired on an Agilent 1200 HPLC system equipped with DAD/ELSD/LSMS-6120 diode matrix and mass-selective detector. Melting points were determined using a Fischer Johns instrument. Elemental analysis was performed at an analytical laboratory of the Institute of Bioorganic Chemistry and Petrochemistry, National Academy of Sciences of Ukraine.

3.2. General Procedure for the Synthesis of 4-Alkyl-4H-furo[3,2-*b*]pyrrole-5-carboxylic Acid 3a,c-f and 4-Alkyl-4H-thieno[3,2-*b*]pyrrole-5-carboxylic Acid 4a-d, f

A solution of methyl 4H-furo[3,2-*b*]pyrrole-5-carboxylate **1** (20 mmol) [40] or methyl 4H-thieno[3,2-*b*]pyrrole-5-carboxylate **2** [41] in DMF (15 mL) was added dropwise at stirring under inert atmosphere to suspension of sodium hydride (1 g, 25 mmol, prepared from

preliminarily washed with anhydrous hexanes 60% suspension of NaH in mineral oil) in DMF (15 mL). The mixture was stirred for 20 min, corresponding alkyl halide (25 mmol) was added, and the mixture was continuously stirred at 45 °C until completion (TLC control by disappearing of initial compound **1** or **2**). After cooling to ambient temperature acetic acid (1 mL) was added and the mixture was evaporated to dryness under reduced pressure. After addition water (50 mL), the formed precipitate was filtered off, dissolved in methanol (30 mL), and treated with a solution of potassium hydroxide (3.36 g, 60 mmol) in water (15 mL). The resulted mixture was stirred at 50 °C for 18 h (TLC control), cooled to ambient temperature, and acidified with formic acid. The formed precipitate was filtered off, washed with water, dried in air, and crystallized from ethanol.

4-Methyl-4*H*-furo[3,2-*b*]pyrrole-5-carboxylic acid (**3a**). Yield 82%; m.p. 158–160 °C. ¹H-NMR (400 MHz, DMSO-*d*₆, ppm) δ 12.29 (s, 1H, COOH), 7.78 (d, *J* = 2.3 Hz, 1H, H-2), 6.78 (d, *J* = 2.3 Hz, 1H, H-3), 6.75 (s, 1H, H-6), 3.91 (s, 3H, NCH₃). ¹³C-NMR (125 MHz, DMSO-*d*₆, ppm) δ 162.90, 148.94, 144.68, 133.21, 124.17, 98.94, 97.59, 34.60. Anal. Calcd. for C₈H₇NO₃ (%): C, 58.18; H, 4.27; N, 8.48 Found (%): C, 58.11; H, 4.31; N, 8.39.

4-Benzyl-4*H*-furo[3,2-*b*]pyrrole-5-carboxylic acid (**3c**). Yield 87%; m.p. 152–154 °C (lit. 129–130. °C [59]). ¹H-NMR (400 MHz, DMSO-*d*₆, ppm) δ 12.35 (s, 1H, COOH), 7.77 (d, *J* = 2.2 Hz, 1H, H-2), 7.35–7.11 (m, 5H, Ar), 6.86 (s, 1H, H-6), 6.68 (d, *J* = 2.2 Hz, 1H, H-3), 5.66 (s, 2H, NCH₂). ¹³C-NMR (125 MHz, DMSO-*d*₆, ppm) δ 162.75, 149.12, 145.00, 138.41, 132.73, 128.47, 127.30, 127.02, 123.63, 99.39, 98.51, 49.62. Anal. Calcd. for C₁₄H₁₁NO₃ (%): C, 69.70; H 4.60; N 5.81 Found (%): C, 69.78; H, 4.54; N, 5.72.

4-(2-Fluorobenzyl)-4*H*-furo[3,2-*b*]pyrrole-5-carboxylic acid (**3d**). Yield 83%; m.p. 162–164 °C. ¹H-NMR (400 MHz, DMSO-*d*₆, ppm) δ 12.39 (s, 1H, COOH), 7.78 (d, *J* = 2.2 Hz, 1H, H-2), 7.35–7.29 (m, 1H, Ar), 7.25–7.17 (m, 1H, Ar), 7.14–7.07 (m, 1H, Ar), 6.88 (s, 1H, H-6), 6.86–6.79 (m, 1H, Ar), 6.56 (d, *J* = 2.2 Hz, 1H, H-3), 5.73 (s, 2H, NCH₂). ¹³C-NMR (125 MHz, DMSO-*d*₆, ppm) δ 162.63, 159.73 (d, *J*_{CF} = 244.9 Hz), 149.18, 144.98, 132.83, 129.46 (d, *J*_{CF} = 8.1 Hz), 128.60 (d, *J*_{CF} = 3.9 Hz), 125.33 (d, *J*_{CF} = 15.0 Hz), 124.62 (d, *J*_{CF} = 3.5 Hz), 123.85, 115.23 (d, *J*_{CF} = 20.9 Hz), 99.27, 98.75, 43.93 (d, *J*_{CF} = 4.6 Hz). Anal. Calcd. for C₁₄H₁₀FNO₃ (%): C, 64.87; H, 3.89; N, 5.40 Found (%): C, 64.79; H, 3.97; N, 5.29.

4-(2-Chlorobenzyl)-4*H*-furo[3,2-*b*]pyrrole-5-carboxylic acid (**3e**). Yield 91%; m.p. 149–152 °C. ¹H-NMR (400 MHz, DMSO-*d*₆, ppm) δ 12.25 (s, 1H, COOH), 7.76 (d, *J* = 2.2 Hz, 1H, H-2), 7.52–7.45 (m, 1H, Ar), 7.35–7.18 (m, 2H, Ar), 6.92 (s, 1H, H-6), 6.57–6.49 (m, 1H, Ar), 6.47 (d, *J* = 2.2 Hz, 1H, H-3), 5.75 (s, 2H, NCH₂). ¹³C-NMR (125 MHz, DMSO-*d*₆, ppm) δ 162.52, 149.21, 145.06, 135.94, 132.80, 131.46, 129.24, 128.92, 127.52, 127.31, 124.08, 99.22, 98.77, 48.01. Anal. Calcd. for C₁₄H₁₀ClNO₃ (%): C, 60.99; H, 3.66; Cl, 12.86; N, 5.08 Found (%): C, 61.10; H, 3.73; Cl, 12.65; N, 5.15.

4-(4-Chlorobenzyl)-4*H*-furo[3,2-*b*]pyrrole-5-carboxylic acid (**3f**). Yield 92%; m.p. 131–132 °C. ¹H-NMR (400 MHz, DMSO-*d*₆, ppm) δ 12.32 (s, 1H, COOH), 7.77 (d, *J* = 2.2 Hz, 1H, H-2), 7.36 (d, *J* = 8.3 Hz, 2H, Ar), 7.16 (d, *J* = 8.3 Hz, 2H, Ar), 6.84 (s, 1H, H-6), 6.69 (d, *J* = 2.2 Hz, 1H, H-3), 5.65 (s, 2H, NCH₂). ¹³C-NMR (125 MHz, DMSO-*d*₆, ppm) δ 162.69, 149.24, 145.00, 137.47, 132.71, 131.92, 128.79, 128.47, 123.54, 99.30, 98.67, 48.94. Anal. Calcd. for C₁₄H₁₀ClNO₃ (%): C, 60.99; H, 3.66; Cl, 12.86; N, 5.08 Found (%): C, 61.13; H, 3.75; Cl, 12.71; N, 5.04.

4-Methyl-4*H*-thieno[3,2-*b*]pyrrole-5-carboxylic acid (**4a**). Yield 88%; m.p. 168–169 °C (lit. 172–174 °C [60]). ¹H-NMR (400 MHz, DMSO-*d*₆, ppm) δ 12.45 (s, 1H, COOH), 7.54 (d, *J* = 5.4 Hz, 1H, H-2), 7.21 (d, *J* = 5.4 Hz, 1H, H-3), 7.11 (s, 1H, H-6), 3.99 (s, 3H, NCH₃). ¹³C-NMR (125 MHz, DMSO-*d*₆, ppm) δ 162.50, 145.45, 129.29, 127.03, 120.73, 111.20, 108.70, 34.40. Anal. Calcd. for C₈H₇NO₂S (%): C, 53.03; H, 3.89; N, 7.73; S, 17.69 Found (%): C, 53.15; H, 3.92; N, 7.61; S, 17.91.

4-Ethyl-4*H*-thieno[3,2-*b*]pyrrole-5-carboxylic acid (**4b**). Yield 83%; m.p. 155–156 °C. ¹H-NMR (400 MHz, DMSO-*d*₆, ppm) δ 12.47 (s, 1H, COOH), 7.55 (d, *J* = 5.4 Hz, 1H, H-2), 7.24 (d, *J* = 5.4 Hz, 1H, H-3), 7.13 (s, 1H, H-6), 4.51 (q, *J* = 7.1 Hz, 2H, NCH₂), 1.29 (t, *J* = 7.1 Hz, 3H, CH₃). ¹³C-NMR (125 MHz, DMSO-*d*₆, ppm) δ 162.25, 144.46, 129.39, 126.05,

120.97, 111.09, 109.03, 41.69, 16.32. Anal. Calcd. for $C_9H_9NO_2S$ (%): C, 55.37; H, 4.65; N, 7.17; S, 16.42 Found (%): C, 55.51; H, 4.72; N, 7.03; S, 16.64.

4-Benzyl-4*H*-thieno[3,2-*b*]pyrrole-5-carboxylic acid (**4c**). Yield 89%; m.p. 180–181 °C (lit. 180–182 °C [61]). 1H -NMR (400 MHz, DMSO- d_6 , ppm) δ 12.36 (s, 1H, COOH), 7.53 (d, J = 5.4 Hz, 1H, H-2), 7.31–7.19 (m, 4H, H-6, Ar), 7.17 (d, J = 5.4 Hz, 1H, H-3), 7.12 (d, J = 7.4 Hz, 2H, Ar), 5.78 (s, 2H, NCH₂). ^{13}C -NMR (125 MHz, DMSO- d_6 , ppm) δ 162.45, 145.14, 138.59, 129.79, 128.49, 127.22, 126.69, 126.48, 121.45, 111.54, 109.63, 49.40. Anal. Calcd. for $C_{14}H_{11}NO_2S$ (%): C, 65.35; H, 4.31; N, 5.44; S, 12.46 Found (%): 65.50; H, 4.42; N, 5.59; S, 12.70.

4-(2-Fluorobenzyl)-4*H*-thieno[3,2-*b*]pyrrole-5-carboxylic acid (**4d**). Yield 86%; m.p. 179–181 °C. 1H -NMR (400 MHz, DMSO- d_6 , ppm) δ 12.49 (s, 1H, COOH), 7.55 (d, J = 5.4 Hz, 1H, H-2), 7.33–7.24 (m, 2H, H-6, Ar), 7.23–7.16 (m, 1H, Ar), 7.13 (d, J = 5.4 Hz, 1H, H-3), 7.09–7.04 (m, 1H, Ar), 6.69–6.63 (m, 1H, Ar), 5.84 (s, 2H, NCH₂). ^{13}C -NMR (125 MHz, DMSO- d_6 , ppm) δ 162.33, 159.53 (d, J_{CF} = 244.8 Hz), 145.25, 129.87, 129.18 (d, J_{CF} = 8.1 Hz), 127.87 (d, J_{CF} = 4.1 Hz), 126.76, 125.65 (d, J_{CF} = 14.6 Hz), 124.62 (d, J_{CF} = 3.4 Hz), 121.54, 115.24 (d, J_{CF} = 21.0 Hz), 111.33, 109.80, 43.76 (d, J_{CF} = 4.8 Hz). Anal. Calcd. for $C_{14}H_{10}FNO_2S$ (%): C, 61.08; H, 3.66; N, 5.09; S, 11.65 Found (%): C, 60.87; H, 3.73; N, 5.17; S, 11.88.

4-(4-Chlorobenzyl)-4*H*-thieno[3,2-*b*]pyrrole-5-carboxylic acid (**4f**). Yield 91%; m.p. 173–174 °C. 1H -NMR (400 MHz, DMSO- d_6 , ppm) δ 10.50 (s, 1H, COOH), 7.58 (d, J = 5.4 Hz, 1H, H-2), 7.35 (d, J = 8.3 Hz, 2H, Ar), 7.23 (d, J = 5.4 Hz, 1H, H-3), 7.22 (s, 1H, H-6), 7.11 (d, J = 8.3 Hz, 2H, Ar), 5.76 (s, 2H, NCH₂). ^{13}C -NMR (125 MHz, DMSO- d_6 , ppm) δ 162.38, 145.02, 137.59, 131.81, 129.89, 128.52, 128.46, 126.44, 121.51, 111.41, 109.71, 48.77. Anal. Calcd. for $C_{14}H_{10}ClNO_2S$ (%): C, 57.64; H, 3.45; Cl, 12.15; S, 10.99 Found (%): C, 57.49; H, 3.53; Cl, 11.97; S, 12.09.

3.3. General Procedure for the Synthesis of 4-Alkyl-4*H*-furo[3,2-*b*]pyrrole-5-carboxyl Chloride **5a,c,f** and 4-Alkyl-4*H*-thieno[3,2-*b*]pyrrole-5-carboxyl Chloride **6a-d,f**

To a stirred solution of compounds **3a,c,f** or **4a-d,f** (5 mmol) in anhydrous toluene (30 mL) thionyl chloride (3 mL) was added. The mixture was heated for 1 h at 80 °C, evaporated to dryness under reduced pressure, the residue was treated with 10 mL of toluene and the resulted mixture was continuously evaporated to dryness under reduced pressure. The residue was dissolved in the boiling mixture (100 mL of cyclohexane and 75 mL of n-heptane), charcoal (0.5 g) was added, and after stirring for 3 min, filtered, evaporated to dryness under reduced pressure to afford **5a,c,f** and **6a-d,f** as light-yellow crystals. These obtained acid chlorides were immediately used for amides **7** and **8** preparation. The compounds **5a,c,f** and **6a-d,f** are quite unstable (**5a,c,f** decomposed after 2 h of standing, **6a-d,f** decomposed after 8h of standing at ambient temperature).

3.4. General Procedure for the Synthesis of *N*-[4-(aminosulfonyl)phenyl]-4-alkyl-4*H*-Furo[3,2-*b*]pyrrole-5-carboxamide **7a,c,f** and *N*-[4-(aminosulfonyl)phenyl]-4-Alkyl-4*H*-thieno[3,2-*b*]pyrrole-5-carboxamide **8a-d,f**

To an ice-water cooled stirred solution of 4-aminobenzenesulfonamide (0.17 g (1 mmol) and of triethylamine (0.11 g, 1.1 mmol) in acetonitrile (5 mL) the solution of compounds **5a,c,f** or **6a-d,f** (1 mmol) in acetonitrile (10 mL) was added. The mixture was stirred for 1 h at ambient temperature and evaporated to dryness under reduced pressure. After the addition of water (15 mL), the formed precipitate was filtered off, dried in air, and crystallized from the DMF:ethanol mixture.

N-[4-(aminosulfonyl)phenyl]-4-methyl-4*H*-furo[3,2-*b*]pyrrole-5-carboxamide (**7a**). Yield 92%; m.p. 273–275 °C. 1H -NMR (400 MHz, DMSO- d_6 , ppm) δ 10.06 (s, 1H, NH), 7.96–7.73 (m, 5H, Ar, H-2), 7.25 (c, 2H, NH₂), 7.12 (c, 1H, H-6, 6.82 (d, J = 2.2 Hz, 1H, H-3), 3.95 (c, 3H, NCH₃). ^{13}C -NMR (125 MHz, DMSO- d_6 , ppm) 161.03, 149.19, 145.05, 142.85, 138.50, 133.26, 126.98, 126.93, 119.84, 99.48, 96.66, 35.37. MS (APCI): m/z = 320.0 [M + H]⁺; m/z = 317.8 [M – H][–]. Anal. Calcd. for $C_{14}H_{13}N_3O_4S$ (%): C, 52.66; H, 4.10; N, 13.16; S, 10.04 Found (%): C, 52.48; H, 4.18; N13.04; S, 10.26.

N-[4-(aminosulfonyl)phenyl]-4-benzyl-4*H*-furo[3,2-*b*]pyrrole-5-carboxamide (**7c**). Yield 87%; m.p. 240–241 °C. ¹H-NMR (400 MHz, DMSO-*d*₆, ppm) δ 10.12 (s, 1H, NH), 7.89 (d, *J* = 8.6 Hz, 2H, Ar), 7.83–7.73 (m, 3H, H-2, Ar), 7.34–7.16 (m, 8H, H-6, Ar, NH₂), 6.69 (d, *J* = 2.2 Hz, 1H, H-3), 5.72 (s, 2H, NCH₂). ¹³C-NMR (125 MHz, DMSO-*d*₆, ppm) δ 160.98, 149.30, 145.47, 142.70, 138.96, 138.59, 132.79, 128.92, 127.76, 127.55, 126.96, 126.57, 119.90, 99.91, 96.68, 50.30. MS (APCI): *m/z* = 396.0 [M + H]⁺; *m/z* = 394.0 [M – H][–]. Anal. Calcd. for C₂₀H₁₇N₃O₄S (%): C, 60.75; H, 4.33; N, 10.63; S, 8.11 Found (%): C, 60.67; H, 4.29; N, 10.49; S, 8.34.

N-[4-(aminosulfonyl)phenyl]-4-(2-fluorobenzyl)-4*H*-furo[3,2-*b*]pyrrole-5-carboxamide (**7d**). Yield 89%; m.p. 240–242 °C. ¹H-NMR (400 MHz, DMSO-*d*₆, ppm) δ 10.15 (s, 1H, NH), 7.86 (d, *J* = 8.7 Hz, 2H, Ar), 7.80–7.74 (m, 3H, H-2, Ar), 7.36–7.17 (m, 5H, H-6, NH₂, Ar), 7.13–7.07 (m, 1H, Ar), 6.95–6.89 (m, 1H, Ar), 6.60 (d, *J* = 2.3 Hz, 1H, H-3), 5.79 (s, 2H, NCH₂). ¹³C-NMR (125 MHz, DMSO-*d*₆, ppm) δ 160.4, 159.76 (d, *J*_{CF} = 245 Hz), 148.87, 144.99, 142.19, 138.19, 132.39, 129.46 (d, *J*_{CF} = 8.1 Hz), 128.81 (d, *J*_{CF} = 4.0 Hz), 126.50, 126.34, 125.39 (d, *J*_{CF} = 14.8 Hz), 124.59 (d, *J*_{CF} = 3.4 Hz), 119.45, 115.25 (d, *J*_{CF} = 20.9 Hz), 99.34, 96.42, 44.14 (d, *J*_{CF} = 4.4 Hz). MS (APCI): *m/z* = 414.0 [M + H]⁺; *m/z* = 412.0 [M – H][–]. Anal. Calcd. for C₂₀H₁₆FN₃O₄S (%): C, 58.10; H, 3.90; N, 10.16; S, 7.76 Found (%): C, 58.18; H, 3.96; N, 9.97; S, 7.89.

N-[4-(aminosulfonyl)phenyl]-4-(2-chlorobenzyl)-4*H*-furo[3,2-*b*]pyrrole-5-carboxamide (**7e**). Yield 93%; m.p. 239–241 °C. ¹H-NMR (400 MHz, DMSO-*d*₆, ppm) δ 10.14 (s, 1H, NH), 7.83 (d, *J* = 8.6 Hz, 2H, Ar), 7.78–7.71 (m, 3H, H-2, Ar), 7.51–7.45 (m, 1H, Ar), 7.38–7.19 (m, 5H, H-6, Ar, NH₂), 6.62–6.57 (m, 1H, Ar), 6.53 (d, *J* = 2.2 Hz, 1H, H-3), 5.80 (s, 2H, NCH₂). ¹³C-NMR (125 MHz, DMSO-*d*₆, ppm) δ 160.75, 149.42, 145.51, 142.58, 138.62, 136.48, 132.88, 131.87, 129.71, 129.37, 127.93, 127.89, 126.93, 126.86, 119.86, 99.77, 96.85, 48.73. MS (APCI): *m/z* = 432.0 ([M(³⁷Cl)+H]⁺; 30); *m/z* = 430.0 ([M(³⁵Cl)+H]⁺, 100); *m/z* = 430.0 ([M(³⁷Cl)-H][–], 30); *m/z* = 428.0 ([M(³⁷Cl)-H][–], 100). Anal. Calcd. for C₂₀H₁₆ClN₃O₄S (%): C, 55.88; H, 3.75; N, 9.77; S, 7.46 Found (%): C, 55.75; H, 3.77; N, 9.92; S, 7.62.

N-[4-(aminosulfonyl)phenyl]-4-(4-chlorobenzyl)-4*H*-furo[3,2-*b*]pyrrole-5-carboxamide (**7f**). Yield 94%; m.p. 237–238 °C. ¹H-NMR (400 MHz, DMSO-*d*₆, ppm) δ 10.13 (s, 1H, NH), 7.87 (d, *J* = 8.7 Hz, 2H, Ar), 7.81–7.74 (m, 3H, H-2, Ar), 7.37 (d, *J* = 8.5 Hz, 2H, Ar), 7.26 (s, 2H, NH₂), 7.24–7.19 (m, 3H, H-6, Ar), 6.76 (d, *J* = 2.2 Hz, 1H, H-3), 5.70 (s, 2H, NCH₂). ¹³C-NMR (125 MHz, DMSO-*d*₆, ppm) δ 160.45, 148.98, 145.04, 142.18, 138.19, 137.57, 132.33, 131.92, 128.93, 128.47, 126.50, 126.00, 119.49, 99.38, 99.36, 49.21. MS (APCI): *m/z* = 432.0 ([M(³⁷Cl)+H]⁺; 30); *m/z* = 430.0 ([M(³⁵Cl)+H]⁺, 100); *m/z* = 429.8 ([M(³⁷Cl)-H][–], 30); *m/z* = 427.8 ([M(³⁷Cl)-H][–], 100). Anal. Calcd. for C₂₀H₁₆ClN₃O₄S (%): C, 55.88; H, 3.75; N, 9.77; S, 7.46 Found (%): C, 55.83; H, 3.71; N, 9.89; S, 7.59.

N-[4-(aminosulfonyl)phenyl]-4-methyl-4*H*-thieno[3,2-*b*]pyrrole-5-carboxamide (**8a**). Yield 95%; m.p. 276–278 °C. ¹H-NMR (400 MHz, DMSO-*d*₆, ppm) δ 10.29 (s, 1H, NH), 7.93 (d, *J* = 8.8 Hz, 2H, Ar), 7.79 (d, *J* = 8.8 Hz, 2H, Ar), 7.55 (d, *J* = 5.4 Hz, 1H, H-2), 7.40 (s, 1H, H-6), 7.31–7.23 (m, 3H, H-3, NH₂), 4.03 (s, 3H, NCH₃). ¹³C-NMR (125 MHz, DMSO-*d*₆, ppm) δ 160.25, 145.13, 142.30, 138.25, 129.65, 128.77, 126.55, 120.53, 119.47, 111.22, 105.87, 34.55. MS (APCI): *m/z* = 336.1 [M + H]⁺; *m/z* = 334.0 [M – H][–]. Anal. Calcd. for C₁₄H₁₃N₃O₃S₂ (%): C, 50.14; H, 3.91; N, 12.53; S, 19.12 Found (%): C, 50.03; H, 3.97; N, 12.32; S, 19.27.

N-[4-(aminosulfonyl)phenyl]-4-ethyl-4*H*-thieno[3,2-*b*]pyrrole-5-carboxamide (**8b**). Yield 88%; m.p. 248–249 °C. ¹H-NMR (400 MHz, DMSO-*d*₆, ppm) δ 10.28 (s, 1H, NH), 7.92 (d, *J* = 8.8 Hz, 2H, Ar), 7.79 (d, *J* = 8.8 Hz, 2H, Ar), 7.55 (d, *J* = 5.4 Hz, 1H, H-2), 7.40 (s, 1H, H-6), 7.30–7.22 (m, 3H, H-3, NH₂), 4.54 (q, *J* = 7.1 Hz, 2H, NCH₂), 1.34 (t, *J* = 7.1 Hz, 3H, CH₃). Anal. Calcd. for C₁₅H₁₅N₃O₃S₂ (%): C, 51.56; H, 4.33; N, 12.03; S, 18.35 Found (%): C, 51.64; H, 4.39; N, 11.89; S, 18.57.

N-[4-(aminosulfonyl)phenyl]-4-benzyl-4*H*-thieno[3,2-*b*]pyrrole-5-carboxamide (**8c**). Yield 87%; m.p. 255–256 °C. ¹H-NMR (400 MHz, DMSO-*d*₆, ppm) δ 10.29 (s, 1H, NH), 7.89 (d, *J* = 8.5 Hz, 2H, Ar), 7.79 (d, *J* = 8.5 Hz, 2H, Ar), 7.53 (d, *J* = 5.3 Hz, 1H, H-2), 7.46 (s, 1H, H-6), 7.31–7.13 (m, 8H, H-3, Ar, NH₂), 5.82 (s, 2H, NCH₂). ¹³C-NMR (125 MHz, DMSO-*d*₆,

ppm) δ 160.25, 144.77, 142.15, 138.62, 138.33, 129.21, 129.18, 128.46, 127.22, 126.80, 126.53, 121.21, 119.49, 111.56, 106.82, 49.54. MS (APCI): $m/z = 412.0$ $[M + H]^+$; $m/z = 409.8$ $[M - H]^-$. Anal. Calcd. for $C_{20}H_{17}N_3O_3S_2$ (%): C, 58.38; H, 4.16; N, 10.21; S, 15.58 Found (%): C, 58.25; H, 4.22; N, 10.32; S, 15.76.

N-[4-(aminosulfonyl)phenyl]-4-(2-fluorobenzyl)-4*H*-thieno[3,2-*b*]pyrrole-5-carboxamide (**8d**). Yield 91%; m.p. 235–237 °C. 1H -NMR (400 MHz, DMSO- d_6 , ppm) δ 10.36 (s, 1H, NH), 7.86 (d, $J = 8.7$ Hz, 2H, Ar), 7.76 (d, $J = 8.7$ Hz, 2H, Ar), 7.55 (d, $J = 5.4$ Hz, 1H, H-2), 7.48 (s, 1H, H-6), 7.30–7.28 (m, 5H, H-3, Ar, NH₂), 7.08–7.02 (m, 1H, Ar), 6.79–6.72 (m, 1H, Ar), 5.88 (s, 2H, NCH₂). MS (APCI): $m/z = 430.0$ $[M + H]^+$; $m/z = 428.0$ $[M - H]^-$. Anal. Calcd. for $C_{20}H_{16}FN_3O_3S_2$ (%): C, 55.93; H, 3.75; N, 9.78; S, 14.93 Found (%): C, 55.79; H, 3.81; N, 9.96; S, 15.14.

N-[4-(aminosulfonyl)phenyl]-4-(4-chlorobenzyl)-4*H*-thieno[3,2-*b*]pyrrole-5-carboxamide (**8f**). Yield 90%; m.p. 219–220 °C. 1H -NMR (400 MHz, DMSO- d_6 , ppm) δ 10.33 (s, 1H, NH), 7.88 (d, $J = 8.6$ Hz, 2H, Ar), 7.78 (d, $J = 8.6$ Hz, 2H, Ar), 7.56 (d, $J = 5.3$ Hz, 1H, H-2), 7.48 (s, 1H, H-6), 7.35 (d, $J = 8.4$ Hz, 2H, Ar), 7.26–7.20 (m, 3H, H-3, NH₂), 7.18 (d, $J = 8.4$ Hz, 2H, Ar), 5.80 (s, 2H, NCH₂). MS (APCI): $m/z = 447.8$ $([M(^{37}Cl)+H]^+; 30)$; $m/z = 446.0$ $([M(^{35}Cl)+H]^+; 100)$; $m/z = 448.8$ $([M(^{37}Cl)-H]^-; 30)$; $m/z = 443.8$ $([M(^{37}Cl)-H]^-; 100)$. Anal. Calcd. for $C_{20}H_{16}ClN_3O_3S_2$ (%): C, 53.87; H, 3.62; N, 9.42; S, 14.38 Found (%): C, 54.01; H, 3.59; N, 9.57; S, 14.60.

3.5. Synthesis of *N*-[4-(aminosulfonyl)phenyl]-2-methyl-3-oxo-3,4-dihydro-2*H*-1,4-benzoxazine-2-carboxamide (**11**)

To a stirred solution of **9** (0.21 g, 1 mmol) [42] in anhydrous toluene (10 mL) thionyl chloride (1 mL) was added. The mixture was heated for 1 h at 80 °C and then evaporated to dryness under reduced pressure, the residue was treated with toluene (5 mL) and the resulted mixture was continuously evaporated to dryness under reduced pressure. The residue was dissolved in acetonitrile (10 mL) and then was added to an ice-water cooled solution of 4-aminobenzenesulfonamide (0.17 g, 1 mmol) and of triethylamine (0.11 g, 1.1 mmol) in acetonitrile. (5 mL). The mixture was stirred for 1 h, evaporated to dryness under reduced pressure. The residue was treated with water (15 mL), the formed precipitate was filtered off, dried in air, and crystallized from the DMF–ethanol mixture (1:3 *v/v*) to afford **11**. Yield 91%; m.p. 269–270 °C. 1H -NMR (400 MHz, DMSO- d_6 , ppm) δ 10.91 (s, 1H, NH), 10.49 (s, 1H, NH), 7.78–7.68 (m, 4H, Ar), 7.24 (s, 2H, NH₂), 7.18–7.12 (m, 1H, Ar), 7.02–6.88 (m, 3H, Ar), 1.73 (s, 3H, CH₃). MS (APCI): $m/z = 362.0$ $[M + H]^+$; $m/z = 360.0$ $[M - H]^-$. Anal. Calcd. for $C_{16}H_{15}N_3O_5S$ (%): C, 53.18; H, 4.18; N, 11.63; S, 8.87 Found (%): C, 53.29; H, 4.15; N, 11.81; S, 9.03.

3.6. Synthesis of *N*-[4-(aminosulfonyl)phenyl]-3-phenyl-5,6-dihydro-1,4-oxathiine-2-carboxamide (**14a**)

To a stirred solution of compound **12** (0.22 g, 1 mmol) [43] in anhydrous benzene (10 mL) thionyl chloride (1 mL) was added. The mixture was stirred at 48–50 °C for 3 h, evaporated to dryness under reduced pressure, the residue was dissolved in acetonitrile (10 mL) and this solution was added to an ice-water cooled solution of 4-aminobenzenesulfonamide (0.17 g, 1 mmol) and triethylamine (0.11 g, 1.1 mmol) in acetonitrile (5 mL). The mixture was stirred for 1 h at ambient temperature and evaporated to dryness under reduced pressure, the residue was treated with water (15 mL), the formed precipitate was filtered off and crystallized from ethanol to afford **14a**. Yield 93%; m.p. 233–235 °C. 1H -NMR (400 MHz, DMSO- d_6 , ppm) δ 10.08 (s, 1H, NH), 7.75–7.67 (m, 4H, Ar), 7.35–7.26 (m, 5H, Ar), 7.23 (s, 2H, NH₂), 4.40–4.35 (m, 2H, OCH₂), 3.32–3.24 (m, 2H, SCH₂). ^{13}C -NMR (125 MHz, DMSO- d_6 , ppm) δ 160.67, 141.98, 139.46, 138.96, 137.69, 129.14, 128.47, 128.25, 126.89, 119.75, 119.07, 64.93, 27.87. MS (APCI): $m/z = 377.1$ $[M + H]^+$; $m/z = 375.0$ $[M - H]^-$. Anal. Calcd. for $C_{17}H_{16}N_2O_4S_2$ (%): C, 54.24; H, 4.28; N, 7.44; S, 17.03 Found (%): C, 54.31; H, 4.34; N, 7.56; S, 17.29.

N-[2-[4-(aminosulfonyl)phenyl]ethyl]-3-phenyl-5,6-dihydro-1,4-oxathiane-2-carboxamide (**14b**), was obtained similarly to **14a**. Yield 87%; m.p. 208–209 °C. ¹H-NMR (400 MHz, DMSO-*d*₆, ppm) δ 7.98 (t, *J* = 5.9 Hz, 1H, NH), 7.73 (d, *J* = 8.3 Hz, 2H, Ar), 7.33–7.15 (m, 9H, Ar, NH₂), 4.32–4.24 (m, 2H, OCH₂), 3.27–3.15 (m, 4H, NHCH₂, OCH₂), 2.73–2.65 (m, 2H, CH₂Ar). ¹³C-NMR (125 MHz, DMSO-*d*₆, ppm) δ 161.85, 144.00, 142.44, 139.94, 138.07, 129.42, 129.23, 128.22, 127.88, 126.1, 116.24, 64.79, 35.00, 27.68. MS (APCI): *m/z* = 405.1 [M + H]⁺; *m/z* = 403.0 [M – H][–]. Anal. Calcd. for C₁₉H₂₀N₂O₄S₂ (%): C, 56.42; H, 4.98; N, 6.93; S, 15.85 Found (%): C, 56.30; H, 5.07; N, 6.85; S, 16.03.

3.7. Synthesis of 4-(5-((Z)-[2-(3-chlorophenyl)-6-oxo[1,3]thiazolo[3,2-b][1,2,4]triazol-5(6H)-ylidene]methyl)-2-furyl)benzenesulfonamide (**17a**)

A solution of compound **15a** (0.42 g, 2 mmol) [44], chloroacetic acid (0.2 g, 2 mmol), 4-(5-formyl-2-furyl) benzenesulfonamide (0.5 g, 2 mmol) **16** [45], and of sodium acetate (0.49 g, 6 mmol) in the mixture of acetic acid (10 mL) and of acetic anhydride (4 mL) was refluxed for 4 h. The reaction mixture was kept overnight, the formed precipitate was filtered off, washed with cool water, dried and crystallized from the DMF:ethanol mixture (1:1 *v/v*) to afford **17a**. Yield 78%; m.p. 312–315 °C. ¹H-NMR (400 MHz, DMSO-*d*₆, ppm) δ 8.14 (s, 1H, CH=), 8.11–7.92 (m, 6H, Ar), 7.58–7.51 (m, 2H, Ar), 7.44–7.14 (m, 2H, Ar), 7.35 (s, 2H, NH₂). Anal. Calcd. for C₂₁H₁₃ClN₄O₄S₂ (%): C, 52.01; H, 2.70; N, 11.55; S, 13.22 Found (%): C, 51.83; H, 2.74; N, 11.72; S, 13.39.

4-(5-((Z)-[2-(3,4-Dimethoxyphenyl)-6-oxo[1,3]thiazolo[3,2-b][1,2,4]triazol-5(6H)-ylidene]methyl)-2-furyl)benzenesulfonamide (**17b**) was obtained similarly to **17a** starting from **15b** [44]. Yield 71%; m.p. 294–295 °C. ¹H-NMR (400 MHz, DMSO-*d*₆, ppm) δ 8.10 (s, 1H, CH=), 8.02 (d, *J* = 8.5 Hz, 2H, Ar), 7.95 (d, *J* = 8.5 Hz, 2H, Ar), 7.67 (d, *J* = 8.4 Hz, 1H, Ar), 7.57 (s, 1H, Ar), 7.44–7.37 (m, 4H, NH₂, Ar), 7.03 (d, *J* = 8.4 Hz, 1H, Ar), 3.86 (s, 3H, OCH₃), 3.84 (s, 3H, OCH₃). ¹³C-NMR (125 MHz, DMSO-*d*₆, ppm) δ 168.36, 160.39, 156.50, 155.71, 151.18, 149.38, 148.78, 144.09, 131.06, 126.68, 124.89, 123.67, 121.34, 120.19, 112.02, 111.65, 109.27, 55.52, 55.37. MS (APCI): *m/z* = 511.0 [M + H]⁺; *m/z* = 509.0 [M – H][–]. Anal. Calcd. for C₂₃H₁₈N₄O₆S₂ (%): C, 54.11; H, 3.55; N, 10.97; S, 12.56 Found (%): C, 53.96; H, 3.62; N, 10.79; S, 12.79.

3.8. Carbonic Anhydrase Inhibition

An Applied Photophysics stopped-flow instrument was used for assaying the CA catalyzed CO₂ hydration activity [61]. Phenol red (at a concentration of 0.2 mM) was used as an indicator, working at the absorbance maximum of 557 nm, with 20 mM Hepes (pH 7.4) as a buffer, and 10 mM Na₂SO₄ (for maintaining constant ionic strength), following the initial rates of the CA-catalyzed CO₂ hydration reaction for a period of 10–100 s. The CO₂ concentrations ranged from 1.7 to 17 mM for the determination of the kinetic parameters and inhibition constants [10]. Enzyme concentrations ranged between 5–12 nM. For each inhibitor, at least six traces of the initial 5–10% of the reaction were used for determining the initial velocity. The uncatalyzed rates were determined in the same manner and subtracted from the total observed rates. Stock solutions of the inhibitor (0.1 mM) were prepared in distilled–deionized water and dilutions up to 0.01 nM were done thereafter with the assay buffer. Inhibitor and enzyme solutions were preincubated together for 15 min at room temperature prior to the assay, allowing the formation of the E–I complex. The inhibition constants were obtained by non-linear least-squares methods using PRISM 3 and the Cheng–Prusoff equation as reported earlier, which represent the mean from at least three different determinations. All CA isoforms were recombinant proteins obtained in-house, as reported earlier [62–65].

3.9. Molecular Modeling Studies

AutoDock 4.2 software was used to perform molecular modeling studies [66]. The crystal structures of the cytosolic isoforms hCA I (PDB code 3W6H) and hCA II (PDB code 3HS4), as well as the transmembrane tumor-associated ones hCA IX (PDB code

3IAI) and hCA XII (PDB code 1JD0) were obtained from the Protein Data Bank [67]. The procedure was carried out as mentioned in our previous work [68]. For the preparation of enzymes, all water molecules were removed, polar hydrogens were added and the co-crystallized ligands were removed from each enzyme's active site. Charges were added and the rotatable bonds determined for preparation of the tested compounds. The autogrid algorithm was used for the calculation of grid maps. A set of grids of 60 Å × 50 Å × 50 Å with 0.375 Å spacing was calculated considering the docking area for all the ligands atom types employing AutoGrid4. Three-dimensional structures of all compounds were constructed using Chem3D Ultra 12.0 software (Chemical Structure Drawing Standard; Perkin Elmer Informatics, Waltham, MA, USA). For the present system, the Lamarckian genetic algorithm was applied for minimization using default parameters. The pitch was 1.0 Å, while the quaternion and pivot angle was set to 5.0 degrees. For each compound, 200 configurations were produced. The results from the Autodock calculations were grouped using a root mean standard deviation (RMSD) value of 1.5 Å, while the lowest-energy configuration of the largest population group was chosen as the most likely tethering configuration. The LigandScout software program was used to display the results and process the configurations with the highest tie rating [68]. Finally, the docking protocol was verified by re-docking of the co-crystallized ligand acetazolamide (AAZ) in the vicinity of the active sites of each enzyme with RMSD values 0.885, 0.966, 1.034, and 1.176 Å for hCA I, II, IX, and XII, respectively.

3.10. In-Silico Predictive Studies

The targeted molecules were appraised for predicting the Drug-likeness based on 5 separate filters namely. Lipinski, Ghose, Veber, Egan, and Muegge [55–60] rules accompanying bioavailability and Drug-likeness scores using the Molsoft software and SwissADME program (<http://swissadme.ch> (accessed on 8 July 2021)) using the ChemAxon's Marvin JS structure drawing tool.

4. Conclusions

In summary, we designed and synthesized fifteen sulfanilamide derivatives bearing different heterocyclic rings (7–17) adopting different synthetic pathways to increase the potency and selectivity. All the synthesized compounds were screened against four CA isoforms, I, II, IX, and XII showing selectivity toward the isoforms hCA II and hCA XII. In addition, in silico studies are performed on the best derivatives (7c, 8a, 8b, 11, and 14), clarifying the mode of interaction within the hCA II and XII binding sites, illustrating the possible interaction with the active site to justify the selective inhibition activity and prospectively guide the future design of more active and isoform-selective CAIs.

Supplementary Materials: The following are available online at <https://www.mdpi.com/article/10.3390/ph14080828/s1>.

Author Contributions: Conceptualization, A.G. and V.K.; methodology, V.B., V.D.L. and C.C.; software, A.P.; formal analysis, R.M.V.; investigation, S.Y.P., A.A. and M.P.; data curation, A.G., V.B. and C.T.S.; original draft preparation, A.G., V.B. and A.A.; review and editing, A.G. and C.T.S.; supervision, A.G. and C.T.S. All authors have read and agreed to the published version of the manuscript.

Funding: This research received no external funding.

Institutional Review Board Statement: Not applicable.

Informed Consent Statement: Not applicable.

Data Availability Statement: Data is contained within the article.

Conflicts of Interest: The authors declare no conflict of interest.

References

1. Supuran, C.T. Emerging role of carbonic anhydrase inhibitors. *Clin. Sci.* **2021**, *135*, 1233–1249. [CrossRef] [PubMed]

2. Xu, Y.; Feng, L.; Jeffrey, P.D.; Shi, Y.; Morel, F.M. Structure and metal exchange in the cadmium carbonic anhydrase of marine diatoms. *Nature* **2008**, *452*, 56–61. [[CrossRef](#)]
3. Capasso, C.; Supuran, C.T. An overview of the alpha-, beta- and gamma-carbonic anhydrases from bacteria: Can bacterial carbonic anhydrases shed new light on evolution of bacteria? *J. Enzym. Inhib. Med. Chem.* **2015**, *30*, 325–332. [[CrossRef](#)]
4. Supuran, C.T.; Capasso, C. The eta-class carbonic anhydrases as drug targets for antimalarial agents. *Expert. Opin. Ther. Targets* **2015**, *19*, 551–563. [[CrossRef](#)]
5. Del Prete, S.; Vullo, D.; De Luca, V.; Supuran, C.T.; Capasso, C. Biochemical characterization of the δ - carbonic anhydrase from the marine diatom *Thalassiosira weissflogii*, TweCA. *J. Enzym. Inhib. Med. Chem.* **2014**, *29*, 906–911. [[CrossRef](#)]
6. Stefanucci, A.; Angeli, A.; Dimmito, M.P.; Luisi, G.; Del Prete, S.; Capasso, C.; Donald, W.A.; Mollica, A.; Supuran, C.T. Activation of β - and γ -carbonic anhydrases from pathogenic bacteria with tripeptides. *J. Enzym. Inhib. Med. Chem.* **2018**, *33*, 945–950. [[CrossRef](#)] [[PubMed](#)]
7. Angeli, A.; Del Prete, S.; Alasmarty, F.A.S.; Alqahtani, L.S.; AlOthman, Z.; Donald, W.A.; Capasso, C.; Supuran, C.T. The first activation studies of the η -carbonic anhydrase from the malaria parasite *Plasmodium falciparum* with amines and amino acids. *Bioorg. Chem.* **2018**, *80*, 94–98. [[CrossRef](#)] [[PubMed](#)]
8. Angeli, A.; Buonanno, M.; Donald, W.A.; Monti, S.M.; Supuran, C.T. The zinc—but not cadmium—containing ζ -carbonic from the diatom *Thalassiosira weissflogii* is potently activated by amines and amino acids. *Bioorg. Chem.* **2018**, *80*, 261–265. [[CrossRef](#)]
9. Supuran, C.T. Structure and function of carbonic anhydrases. *Biochem. J.* **2016**, *473*, 2023–2032. [[CrossRef](#)]
10. Supuran, C.T. Carbonic anhydrases: Novel therapeutic applications for inhibitors and activators. *Nat. Rev. Drug Discov.* **2008**, *7*, 168–181. [[CrossRef](#)]
11. Supuran, C.T. Exploring the multiple binding modes of inhibitors to carbonic anhydrases for novel drug discovery. *Expert Opin. Drug Discov.* **2020**, *15*, 671–686. [[CrossRef](#)]
12. Supuran, C.T. Carbonic anhydrases as drug targets—an overview. *Curr. Top. Med. Chem.* **2007**, *7*, 825–833. [[CrossRef](#)]
13. Aggarwal, M.; Boone, C.D.; Kondeti, B.; McKenna, R. Structural annotation of human carbonic anhydrases. *J. Enzym. Inhib. Med. Chem.* **2013**, *28*, 267–277. [[CrossRef](#)]
14. Supuran, C.T. Applications of carbonic anhydrases inhibitors in renal and central nervous system diseases. *Expert. Opin. Ther. Pat.* **2018**, *28*, 713–721. [[CrossRef](#)] [[PubMed](#)]
15. Supuran, C.T. Carbonic anhydrase inhibitors as emerging agents for the treatment and imaging of hypoxic tumors. *Expert. Opin. Investig. Drugs* **2018**, *27*, 963–970. [[CrossRef](#)] [[PubMed](#)]
16. Scozzafava, A.; Supuran, C.T. Glaucoma and the applications of carbonic anhydrase inhibitors. *Subcell. Biochem.* **2014**, *75*, 349–359.
17. Carta, F.; Dumy, P.; Supuran, C.T.; Winum, J.Y. Multivalent Carbonic Anhydrases Inhibitors. *Int. J. Mol. Sci.* **2019**, *20*, 5352. [[CrossRef](#)]
18. Bozdog, M.; Altamimi, A.S.A.; Vullo, D.; Supuran, C.T.; Carta, F. State of the Art on Carbonic Anhydrase Modulators for Biomedical Purposes. *Curr. Med. Chem.* **2019**, *26*, 2558–2573. [[CrossRef](#)]
19. Peng, W.; Peltier, D.C.; Larsen, M.J.; Kirchoff, P.D.; Larsen, S.D.; Neubig, R.R.; Miller, D.J. Identification of Thieno[3,2-*b*]Pyrrole Derivatives as Novel Small Molecule Inhibitors of Neurotropic Alphaviruses. *J. Infect. Dis.* **2009**, *199*, 950–957. [[CrossRef](#)] [[PubMed](#)]
20. Vianello, P.; Sartori, L.; Amigoni, F.; Cappa, A.; Fagá, G.; Fattori, R.; Legnaghi, E.; Ciossani, G.; Mattevi, A.; Meroni, G.; et al. Thieno[3,2-*b*]pyrrole-5-carboxamides as New Reversible Inhibitors of Histone Lysine Demethylase KDM1A/LSD1. Part 2: Structure-Based Drug Design and Structure-Activity Relationship. *J. Med. Chem.* **2017**, *60*, 1693–1715. [[CrossRef](#)] [[PubMed](#)]
21. Ching, K.C.; Tran, T.; Amrun, S.; Kam, Y.; Ng, L.; Chai, C. Structural Optimizations of Thieno[3,2-*b*]pyrrole Derivatives for the Development of Metabolically Stable Inhibitors of Chikungunya Virus. *J. Med. Chem.* **2017**, *60*, 3165–3186. [[CrossRef](#)]
22. Mohamed, M.S.; El-Domany, R.A.; Abd El-Hameed, R.H. Synthesis of certain pyrrole derivatives as antimicrobial agents. *Acta Pharm.* **2009**, *59*, 145–158. [[CrossRef](#)] [[PubMed](#)]
23. Alizadeh, M.; Jalal, M.; Hamed, K.; Saber, A.; Kheirouri, S.; Pourteymour Fard Tabrizi, F.; Kamari, N. Recent Updates on Anti-Inflammatory and Antimicrobial Effects of Furan Natural Derivatives. *J. Inflamm. Res.* **2020**, *13*, 451–463. [[CrossRef](#)] [[PubMed](#)]
24. Malladi, S.; Nadh, R.V.; Babu, K.S.; Babu, P.S. Synthesis and antibacterial activity studies of 2,4-di substituted furan derivatives. *Beni Suef Univ. J. Basic Appl. Sci.* **2017**, *6*, 345–353. [[CrossRef](#)]
25. Fang, B.; Hu, C.; Ding, Y.; Qin, H.; Luo, Y.; Xu, Z.; Meng, J.; Chen, Z. Discovery of 4*H*-thieno[3,2-*b*]pyrrole derivatives as potential anticancer agents. *J. Heterocyclic Chem.* **2021**, *58*, 1610. [[CrossRef](#)]
26. Archana, P.S.; Chawla, P.A. Thiophene-based derivatives as anticancer agents. An overview on decade's work. *Bioorg. Chem.* **2020**, *101*, 104026. [[CrossRef](#)]
27. Lashin, W.H.; Nassar, I.F.; El Farargy, A.F.; Abdelhamid, A.O. Synthesis of New Furanone Derivatives with Potent Anticancer Activity. *Russ. J. Bioorg. Chem.* **2020**, *46*, 1074–1086. [[CrossRef](#)]
28. Kumar, P.R.; Raju, S.; Goud, P.S.; Sailaja, M.; Sarma, M.R.; Reddy, G.O.; Kumar, M.P.; Reddy, V.V.; Suresh, T.; Hegde, P. Synthesis and biological evaluation of thiophene [3,2-*b*] pyrrole derivatives as potential anti-inflammatory agents. *Bioorg. Med. Chem.* **2004**, *12*, 1221–1230. [[CrossRef](#)]

29. Abd El-Hameed, R.H.; Mahgoub, S.; El-Shanbaky, H.M.; Mohamed, M.S.; Ali, S.A. Utility of novel 2-furanones in synthesis of other heterocyclic compounds having anti-inflammatory activity with dual COX2/LOX inhibition. *J. Enzym. Inhib. Med. Chem.* **2021**, *36*, 977–986. [[CrossRef](#)]
30. Mohamed, M.S.; Ali, S.A.; Abdelaziz, D.H.; Fathallah, S.S. Synthesis and evaluation of novel pyrroles and pyrrolopyrimidines as anti-hyperglycemic agents. *BioMed Res. Int.* **2014**, *2014*, 249780–249793. [[CrossRef](#)]
31. Baldwin, J.J.; Ponticello, G.S.; Anderson, P.S.; Christy, M.E.; Murcko, M.A.; Randall, W.C.; Schwam, H.; Sugrue, M.F.; Springer, J.P.; Gautheron, P. Thienothiopyran-2-sulfonamides: Novel topically active carbonic anhydrase inhibitors for the treatment of glaucoma. *J. Med. Chem.* **1989**, *32*, 2510–2513. [[CrossRef](#)] [[PubMed](#)]
32. Rakesh, K.P.; Wang, S.M.; Leng, J.; Ravindar, L.; Asiri, A.M.; Marwani, H.M.; Qin, H.L. Recent Development of Sulfonyl or Sulfonamide Hybrids as Potential Anticancer Agents: A Key Review. *Anticancer Agents Med. Chem.* **2018**, *18*, 488–505. [[CrossRef](#)] [[PubMed](#)]
33. Kachaeva, M.V.; Hodyna, D.M.; Semenyuta, I.V.; Pilyo, S.G.; Prokopenko, V.M.; Kovalishyn, V.V.; Metelytsia, L.O.; Brovarets, V.S. Design, synthesis and evaluation of novel sulfonamides as potential anticancer agents. *Comput. Biol. Chem.* **2018**, *74*, 294–303. [[CrossRef](#)]
34. Abbas, H.S.; Abd El-Karim, S.S.; Abdelwahed, N.A.M. Synthesis and biological evaluation of sulfonamide derivatives as antimicrobial agents. *Acta Pol. Pharm.* **2017**, *74*, 849–860.
35. Azzam, R.A.; Elsayed, R.E.; Elgemeie, G.H. Design, Synthesis, and Antimicrobial Evaluation of a New Series of N-Sulfonamide 2-Pyridones as Dual Inhibitors of DHPS and DHFR Enzymes. *ACS Omega* **2020**, *5*, 10401–10414. [[CrossRef](#)]
36. Hussein, E.M.; Al-Rooqi, M.M.; Abd El-Galil, S.M.; Ahmed, S.A. Design, synthesis, and biological evaluation of novel N4-substituted sulfonamides: Acetamides derivatives as dihydrofolate reductase (DHFR) inhibitors. *BMC Chem.* **2019**, *13*, 91. [[CrossRef](#)]
37. Ingle, R.G.; Marathe, R.P. Sulfonamido Quinoxalines—Search for anti-inflammatory Agents. *IJPRAS* **2012**, *1*, 46–51.
38. Markowicz-Piasecka, M.; Huttunen, K.M.; Broncel, M.; Sikora, I. Sulfenamide and Sulfonamide Derivatives of Metformin—A New Option to Improve Endothelial Function and Plasma Haemostasis. *Sci. Rep.* **2019**, *9*, 6573–6592. [[CrossRef](#)]
39. Bhuva, N.H.; Talpara, P.K.; Singala, P.M.; Gothaliya, V.K.; Shah, V.H. Synthesis and biological evaluation of pyrimidinyl sulphonamide derivatives as promising class of antitubercular agents. *J. Saudi Chem. Soc.* **2017**, *21*, 517–527. [[CrossRef](#)]
40. O'Brien, A.G.; Lévesque, F.; Seeberger, P.H. Continuous flow thermolysis of azidoacrylates for the synthesis of heterocycles and pharmaceutical intermediates. *Chem. Commun.* **2011**, *47*, 2688–2690. [[CrossRef](#)]
41. Yarovenko, V.N.; Semenov, S.L.; Zavarzin, I.V.; Ignatenko, A.V.; Krayushkin, M.M. Regioselective acylation of methyl 2-methyl-4H-thieno[3,2-b]pyrrole-5-carboxylate. *Russ. Chem. Bull.* **2003**, *52*, 451–456. [[CrossRef](#)]
42. Suhadolc, E.; Urleb, U.; Žbontar, U.; Kikelj, D. A convenient synthesis of 3,4-dihydro-2-methyl-3-oxo-2H-1,4-benzoxazine-2-carboxylic acids and 3,4-dihydro-2-methyl-3-oxo-2H-pyrido[3,2-b]-1,4-oxazine-2-carboxylic acid. *J. Heterocycl. Chem.* **1993**, *30*, 597–602. [[CrossRef](#)]
43. Mamedov, V.A.; Sibgatullina, F.G.; Gubskaya, V.P.; Gainullin, R.M.; Shagidullin, R.R.; Il'yasov, A.V. Synthesis of some new derivatives of dithiene-and oxathienecarboxylic acids. *Chem. Heterocycl. Compd.* **1994**, *30*, 1029–1033. [[CrossRef](#)]
44. Murty, M.S.R.; Ram, K.R.; Rao, B.R.; Rao, R.V.; Katiki, M.R.; Rao, J.V.; Pamanji, R.; Velatooru, L.R. Synthesis, characterization, and anticancer studies of S and N alkyl piperazine-substituted positional isomers of 1,2,4-triazole derivatives. *Med. Chem. Res.* **2014**, *23*, 1661–1671. [[CrossRef](#)]
45. Kozlov, N.G.; Zhikharko, Y.D.; Lytvyn, R.Z.; Gorak, Y.I.; Skakovskii, E.D.; Baranovskii, A.V.; Basalaeva, L.I.; Obushak, M.D. Synthesis of 12-hetaryl-9,9-dimethyl-7,8,9,10-tetrahydrobenzo[a]acridin-11(12H)-ones. *Russ. J. Org. Chem.* **2014**, *50*, 833–839. [[CrossRef](#)]
46. Karthikeyan, M.S.; Holla, B.S. Synthesis, antiinflammatory and antimicrobial activities of some 2,4-dichloro-5-fluorophenyl substituted arylidenetriazolothiazolidinones. *Monatsh. Chem.* **2008**, *139*, 691–696. [[CrossRef](#)]
47. Tozkoparan, B.; Kılıçgilb, G.A.; Ertanb, R.; Ertana, M.; Kelicen, P.; Demirdamar, R. Synthesis and evaluation of anti-inflammatory activity of some thiazolo[3,2-b]-1,2,4-triazole-5(6H)-ones and their Michael addition products. *Arzneim. Forsch.* **1999**, *49*, 1006–1011. [[CrossRef](#)]
48. Rzhavskii, A.A.; Gerasimova, N.P.; Alov, E.M.; Kozlova, O.S.; Danilova, A.S.; Khapova, S.A.; Suponitskii, K.Y. Condensation of 5-(4-methylphenyl)-2,4-dihydro-3H-1,2,4-triazole-3-thione with haloacetic acids. *Russ. Chem. Bull.* **2012**, *61*, 2133–2136. [[CrossRef](#)]
49. Koysal, Y.; Isik, S.; Dogdas, E.; Tozkoparan, B.; Ertan, M. 6-(2-Fluorobenzylidene)-2-[1-(2-fluoro-4-biphenyl)ethyl]thiazolo[3,2-b][1,2,4]triazol-5(6H)-one. *Acta Crystallogr. Sect. C* **2004**, *60*, 356–357. [[CrossRef](#)]
50. Ottana', R.; Maccari, R.; Barreca, M.L.; Bruno, G.; Rotondo, A.; Rossi, A.; Chiricosta, G.; Di Paola, R.; Sautebin, L.; Cuzzocrea, S.; et al. 5-Arylidene-2-imino-4-thiazolidinones: Design and synthesis of novel anti-inflammatory agents. *Bioorg. Med. Chem.* **2005**, *13*, 4243–4252. [[CrossRef](#)]
51. Alterio, V.; Hilvo, M.; Di Fiore, A.; Supuran, C.T.; Pan, P.; Parkkila, S.; Scaloni, A.; Pastorek, J.; Pastorekova, S.; Pedone, C.; et al. Crystal structure of the catalytic domain of the tumor associated human carbonic anhydrase IX. *Proc. Natl. Acad. Sci. USA* **2009**, *106*, 16233–16238. [[CrossRef](#)] [[PubMed](#)]
52. Di Fiore, A.; Truppo, E.; Supuran, C.T.; Alterio, V.; Dathan, N.; Booterabi, F.; Parkkila, S.; Monti, S.M.; De Simone, G. Crystal structure of the C183S/C217S mutant of human CA VII in complex with acetazolamide. *Bioorg. Med. Chem. Lett.* **2010**, *20*, 5023–5026. [[CrossRef](#)]

53. Whittington, D.A.; Waheed, A.; Ulmasov, B.; Shah, G.N.; Grubb, J.H.; Sly, W.S.; Christianson, D.W. Crystal structure of the dimeric extracellular domain of human carbonic anhydrase XII, a bitopic membrane protein overexpressed in certain cancer tumor cells. *Proc. Natl. Acad. Sci. USA* **2001**, *98*, 9545–9550. [CrossRef]
54. Kanamori, K.; Roberts, J.D. Nitrogen-15 nuclear magnetic resonance study of benzenesulfonamide and cyanate binding to carbonic anhydrase. *Biochemistry* **1983**, *22*, 2658–2664. [CrossRef]
55. Lipinski, C.A. Lead- and drug-like compounds: The rule-of-five revolution. *Drug Discov. Today Technol.* **2004**, *1*, 337–341. [CrossRef] [PubMed]
56. Egan, W.J.; Merz, K.M.; Baldwin, J.J. Prediction of drug absorption Using multivariate statistics. *J. Med. Chem.* **2000**, *43*, 3867–3877. [CrossRef]
57. Ghose, A.K.; Viswanadhan, V.N.; Wendoloski, J.J. A knowledge-based approach in designing combinatorial or medicinal chemistry libraries for drug discovery. 1. A qualitative and quantitative characterization of known drug databases. *J. Comb. Chem.* **1999**, *1*, 55–68. [CrossRef]
58. Muegge, I.; Heald, S.L.; Brittelli, D. Simple selection criteria for drug-like chemical matter. *J. Med. Chem.* **2001**, *44*, 1841–1846. [CrossRef]
59. Veber, D.F.; Johnson, S.R.; Cheng, H.Y.; Smith, B.R.; Wars, K.W.; Kopple, K.D. Molecular properties that influence the oral bioavailability of drug candidates. *J. Med. Chem.* **2002**, *45*, 2615–2623. [CrossRef]
60. Khalifah, R.G. The carbon dioxide hydration activity of carbonic anhydrase. I. Stop flow kinetic studies on the native human isoenzymes B and C. *J. Biol. Chem.* **1971**, *246*, 2561–2573. [CrossRef]
61. Bonardi, A.; Falsini, M.; Catarzi, D.; Varano, F.; Di Cesare Mannelli, L.; Tenci, B.; Ghelardini, C.; Angeli, A.; Supuran, C.T.; Colotta, V. Structural investigations on coumarins leading to chromeno[4,3-c]pyrazol-4-ones and pyrano[4,3-c]pyrazol-4-ones: New scaffolds for the design of the tumor-associated carbonic anhydrase isoforms IX and XII. *Eur. J. Med. Chem.* **2018**, *146*, 47–59. [CrossRef]
62. Angeli, A.; Peat, T.S.; Bartolucci, G.; Nocentini, A.; Supuran, C.T.; Carta, F. Intramolecular oxidative deselenization of acylselenoureas: A facile synthesis of benzoxazole amides and carbonic anhydrase inhibitors. *Org. Biomol. Chem.* **2016**, *14*, 11353–11356. [CrossRef]
63. Angeli, A.; Di Cesare Mannelli, L.; Lucarini, E.; Peat, T.S.; Ghelardini, C.; Supuran, C.T. Design, synthesis and X-ray crystallography of selenides bearing benzenesulfonamide moiety with neuropathic pain modulating effects. *Eur. J. Med. Chem.* **2018**, *154*, 210–219. [CrossRef] [PubMed]
64. Angeli, A.; Ferraroni, M.; Supuran, C.T. Famotidine, an antiulcer agent, strongly inhibits helicobacter pylori and human carbonic anhydrases. *ACS Med. Chem. Lett.* **2018**, *9*, 1035–1038. [CrossRef] [PubMed]
65. Angeli, A.; Carta, F.; Bartolucci, G.; Supuran, C.T. Synthesis of novel acyl selenoureido benzenesulfonamides as carbonic anhydrase I, II, VII and IX inhibitors. *Bioorg. Med. Chem.* **2017**, *25*, 3567–3573. [CrossRef] [PubMed]
66. Morris, G.M.; Huey, R.; Lindstrom, W.; Sanner, M.F.; Belew, R.K.; Goodsell, D.S.; Olson, A.J. Autodock4 and AutoDockTools4: Automated docking with selective receptor flexibility. *J. Comput. Chem.* **2009**, *16*, 2785–2791. [CrossRef]
67. A Structural View of Biology. Available online: <http://www.rcsb.org/> (accessed on 8 June 2021).
68. Wolber, G.; Langer, T. LigandScout: 3-D pharmacophores derived from protein-bound ligands and their use as virtual screening filters. *J. Chem. Inf. Model.* **2005**, *45*, 160–169. [CrossRef] [PubMed]